7.72 — mechanika ciała stałego

Piotr Perzyna

STABILITY OF FLOW PROCESSES FOR DISSIPATIVE SOLIDS WITH INTERNAL IMPERFECTIONS

27/1983

WARSZAWA 1983

ISSN 0208-5658

Praca wpłynęła do Redakcji dnia 4 maja 1983 r.

IPPT PAN

N a   p r a w a c h   r ę k o p i s u

Instytut Podstawowych Problemów Techniki PAN

Nakład 170 egz. Ark.wyd. 3. Ark. druk. 4,25.
Oddano do drukarni w czerwcu 1983 r.
Nr zamówienia 704/83   M - 24.

Warszawska Drukarnia Naukowa, Warszawa,
ul.Śniadeckich 8

PIOTR PERZYNA
Institute of Fundamental Technological Research
Polish Academy of Sciences, Warsaw, Poland

STABILITY OF FLOW PROCESSES FOR DISSIPATIVE SOLIDS WITH INTERNAL IMPERFECTIONS

CONTENTS

1. Introduction

The main objective of the paper is to study the onset of the instability of flow process for dissipative bodies with internal imperfections.

Formulation of a quasi-static, isothermal flow process for a bounded body is given. Criteria of localization of plastic deformations are considered.

It has been proved that to describe the postcritical behaviour for dissipative solids we need very precise constitutive modelling and to take into consideration important cooperative effects such as internal imperfections, strain rate sensitivity, etc. So, the constitutive modelling for description of instability and postcritical behaviour is one of the main problems in modern research in the mechanics of solids.

In this paper the constitutive modelling is developed within the framework of two material structures, namely the internal state variable and rate type material structures.

As main effect we would like to include in the description is the influence of internal imperfections and transport phenomena governing the evolution of imperfections in time and its distribution in a body during the flow process. Physical and experimental motivations for these effects are given and theoretical proposition describing the nucleation, growth and diffusion of voids is presented.

Recent experimental investigations for metals at temperatures above 0,3 of the absolute melting point have shown that thermally activated rate processes are significant. The mechanisms of flow and fracture are influenced by strain rate effect, temperature dependence and by kinetics of crack growth. The concentration of the internal imperfections /crack at grain interfaces, voids nucleating on grain boundaries/ in a material during the straining process of a body does depend on the boundary conditions. The transport phenomenon of imperfections during the deformation process plays an important role and frequently has a predominant influence on the onset of instability and, consequently, on the fracture mechanism.

A simple model of an elastic-viscoplastic material with internal imperfections is proposed. This model is justified by physical mechanisms of polycrystalline matter flow in some regions of temperature and strain rate changes. The thermo-activated mechanism causes elastic-viscoplastic flow and the mechanisms of void nucleation and growth plus its diffusion field insert evolution of imperfections in a solid considered. To describe this model a set of the internal state variables $\alpha(\cdot,t)=\{\underset{\sim}{E}_p(\cdot,t), \varkappa(\cdot,t), \xi(\cdot,t)\}$ is introduced, where $\underset{\sim}{E}_p(\cdot,t)$ is interpreted as the inelastic strain tensor field, $\varkappa(\cdot,t)$ as the isotropic work hardening parameter field and ξ as the scalar measure field of the concentration of voids. It is postulated that the evolution equation for ξ has the form of the diffusion equation.

A model proposed has some important features. First, by introducing the control function /control vector/ the model can describe the properties of a material in a range of strain rates near the static value. This model satisfies also the requirement that during the deformation process in which the effective strain rate is equal to the static value the response of a material becomes elastic-plastic. Second, it can describe the evolution of imperfections during the deformation process by taking account of the nucleation of voids as well as the growth of voids. Third, it includs in the description the diffusional accommodated flow mechanism.

The identification procedure for all material functions and constants has been based on available experimental data. Two kinds of experimental tests have been used. First, the mechanical test data for broad range of strain rate changes are utilized to determine material functions and constants in the evolution equations for the inelastic strain tensor $\underset{\sim}{E}_p$ and for the work hardening parameter $\varkappa$. Second, the physical, metallurgical observations are assumed as a basis for determinations material functions and constants in the evolution equation for the concentration of imperfections ξ.

As an example of a quasi-static, isothermal flow process the boundary-initial-value problem describing necking phenomenon has been considered. The problem is formulated in such a way that enables discussion of influence on the onset of localization the strain rate effect, as well as imperfections and diffusion effects. Comparison of theoretical predictions with available experimental results is given.

2. Quasi-static, isothermal flow process for dissipative solids

To describe the flow process for dissipative solids with internal imperfections induced by the nucleation and growth of voids in the material we utilize the modified material structure with internal state variables. We shall postulate that the evolution equations for some of the internal state variables have the form of the partial differential equations. This material structure is sufficiently general to include such cooperative effects like strain rate sensitivity and diffusion processes for kinetics of voids /imperfections/.

So, the quasi-static, isothermal flow process for dissipative solids with internal imperfections will be determined in the material description by

(i) the constitutive equation for the Piola-Kirchhoff stress tensor

$$\underset{\sim}{T} = \underset{\sim}{T}(\sigma), \tag{2.1}$$

where σ denotes the intrinsic state which is given by the pair - the strain tensor field $\underset{\sim}{E}$ and the field of the internal state vector α, i.e.

$$\sigma = (\underset{\sim}{E}, \alpha) \in \Sigma \tag{2.2}$$

and Σ denotes the intrinsic state space.

Basing on the previous results (cf. Rfs. [35-38]) we can write

$$\underset{\sim}{T} = 2\rho_0 \partial_{\underset{\sim}{E}} \hat{\Psi}(\bar{\sigma}), \tag{2.3}$$

where Ψ denotes the free energy constitutive function and ρ_0 is the mass density in the reference configuration;

The intrinsic state $\bar{\sigma} = (\underset{\sim}{E}, \alpha_1)$ does depend on the internal state variables α_1 which are described by the ordinary differential evolution equations and it is independent of the internal state variables α_2 which are described by the partial differential evolution equations. This result yields from the thermodynamic restriction (cf. Ref. [14]) and has very important consequences on the constitutive modelling.

(ii) the evolution equation for the internal state variable vector α in the form

$$\partial_t \alpha(x,t) = \mathcal{L}\alpha(x,t) + \hat{f}(\sigma), \tag{2.4}$$

where $\mathcal{L}$ is a linear spatial differential operator, $\hat{f}$ is a nonlinear function of σ and ∂_t denotes the differentiation with respect to time ;

(iii) the equation for the strain tensor $\underset{\sim}{E}$, i.e.

$$\underset{\sim}{E} = \frac{1}{2}(\underset{\sim}{H} + \underset{\sim}{H}^T + \underset{\sim}{H}\underset{\sim}{H}^T) , \tag{2.5}$$

where $\underset{\sim}{H} = \nabla_X \underset{\sim}{u}$ denotes the displacement gradient ;

(iv) the equilibrium equation

$$\mathrm{Div}\,(\underset{\sim}{F}\underset{\sim}{T}) = 0 , \tag{2.6}$$

where $\underset{\sim}{F}$ is the deformation gradient field ;

(v) the initial values

$$\underset{\sim}{u}(X,0) = 0 , \quad \underset{\sim}{v}(X,0) = \underset{\sim}{v}^{o}(X) , \alpha(X,0) = \alpha^{o}(X) \tag{2.7}$$

for $X \in B$, where $\underset{\sim}{v} = \partial_t \underset{\sim}{u}$ is the velocity vector field ;

(vi) the boundary conditions

$$\begin{aligned} &\underset{\sim}{u}(X,t) = \underset{\sim}{u}^1(X,t) , \\ &a\partial_{\underset{\sim}{n}}\alpha(X,t) + b\,\alpha(X,t) = 0 \end{aligned} \tag{2.8}$$

for $(X,t) \in \partial B \times [0,d_p]$, where $\underset{\sim}{n}$ is the unit outward normal vector on ∂B, $\underset{\sim}{u}^1$, a and b are bounded functions on $\partial B \times [0,d_p]$.

By the solution $\underset{\sim}{\varphi} = \{\underset{\sim}{u}, \alpha\}$ of the quasi-static, isothermal flow process formulated we understand such functions $\underset{\sim}{u}$ and α which satisfy the equations (2.1) - (2.6) with the initial-boundary value conditions (2.7) -(2.8) .

3. Criteria of localization of plastic deformations

The criteria of the onset of instability of the flow process for solids can be considered from two point of views. The first is purely mathematical in nature and can be achieved within the framework of investigation of discontinuous[1/] solution or bifurcation[2/] branching of the solution. The second is more engineering

---

1/ The criteria of discontinuous solution for a flow process have been discussed basing on the first and second Liapounov methods in Ref. [37] .

2/ The criteria of bifurcation have been broadly investigated by HILL [19,20] HILL and HUTCHINSON [22] cf. also the review papers by HILL [21], MILES [27] and ASARO [4] .

approach and is based on investigation of the load-extention curve during a flow process.

During plastic flow processes for dissipative solids the onset of instability is usually connected with the localization of plastic deformations / c.f. RICE [43] and Ref. [36]/.

The most widely recognized mode of localization of plastic deformations is that of necking. A necessary condition for the occurrence of necking are the fluctuations in cross-sectional area. This leads to a maximum load criterion for the instability condition (c.f. CHAKRABARTI and SPRETNAK [9]).

A second basic mode of localization is the phenomenon of plastic instability in direction of pure shear. A necessary condition for the localization of plastic deformations in the form of the plastic shear band is a maximum true flow stress criterion[3/].

In this paper we would like to study necking phenomenon for dissipative solids with internal imperfections and to use the criterion of maximum load as a fundamental condition for the onset of instability.

It is noteworthy that experimental as well as theoretical studies of necking phenomena showed that some additional cooperative effects can influence the onset of instability by shifting the point of initiation of localization from the maximum load point on the load-extention curve[4/].

NEEDLEMAN and RICE [29] have proved that the onset of localization does depend critically on the assumed constitutive law. This means that the onset of instability is influenced not only by the geometry and boundary conditions of the body considered but also by the properties of the material.

In this study we focus mostly on the description of postcritical behaviour of solids, so, the influence of the criterion of localization by different cooperative effects and material properties needs further investigations.

3/ Experimental observations of this criterion were conducted by CHAKRABARTI and SPRETNAK [9]. For recent investigations in this subject see the review papers by PERICE, ASARO and NEEDLEMAN [31] and ASARO [4].

4/ For discussion of these effects see the review papers by PEIRCE, ASARO and NEEDLEMAN [31] and ASARO [4].

4. Constitutive modelling

4.1. Internal state variable material structure. The analysis of thermodynamic restrictions on constitutive assumptions[5/] showed that it is convenient to split the internal state variables α into two groups α_1 and α_2 in such a way that the first group α_1 is described by the ordinary differential evolution equations and the second group α_2 is described by the partial differential evolution equations, c.f. discussion on this subject given in Section 2. So, the intrinsic state has now the form

$$\sigma_1(\cdot,t) = (\underset{\sim}{E}(\cdot,t),\ \alpha_1(\cdot,t),\ \alpha_2(\cdot,t)) \qquad (4.1)$$

FRISCHMUTH and PERZYNA [14] have proved that the internal state variables of the second group α_2 do not influence explicitly the stress. Taking advantage of this result we can write (cf. Eq. (2.3))

$$\underset{\sim}{T} = \hat{\underset{\sim}{T}}(\underset{\sim}{E}(\cdot,t),\ \alpha_1(\cdot,t)) \qquad (4.2)$$

The evolution equations can be written in the form as follows

$$\partial_t \alpha_1(\cdot,t) = \hat{f}_1(\sigma_1(\cdot,t))$$
$$(4.3)$$
$$\partial_t \alpha_2(\cdot,t) = \mathcal{L}\,\alpha_2(\cdot,t) + \hat{f}_2(\sigma_1(\cdot,t)),$$

where $\mathcal{L}$ denotes the spatial differential operator.

The constitutive equation for the stress tensor (4.2) and the evolution equations (4.3) describe the properties of the material of a body if we give the initial values

$$\alpha_1(X,0) = \overset{o}{\alpha}_1(X),\ \alpha_2(X,0) = \overset{o}{\alpha}_2(X) \text{ for } X \in B \qquad (4.4)$$

5/ The investigation of the thermodynamic restrictions for the modified material structure with internal state variables has been presented by FRISCHMUTH and PERZYNA [14].

and the boundary condition

$$a\,\partial_n\,\alpha_2(X,t) + b\,\alpha_2(X,t) = 0$$

$$\text{for } (X,t) \in (\partial B \times [0,d_p]) \qquad (4.5)$$

The thermodynamic condition that the constitutive stress function $\hat{\underset{\sim}{T}}$ does not depend on α_2 is of great importance to constitutive modelling. The consequences of this condition we shall show better when we shall pass to the rate type material structure. To do this we need to specify more directly the both groups of the internal state variables. We postulate

$$\alpha_1(\cdot,t) = (\underset{\sim}{E}_p(\cdot,t),\ \varkappa(\cdot,t)),$$
$$\alpha_2(\cdot,t) = \xi(\cdot,t), \qquad (4.6)$$

where $\underset{\sim}{E}_p(\cdot,t)$ denotes the inelastic strain tensor field, $\varkappa(\cdot,t)$ is the work hardening parameter field, and $\xi(\cdot,t)$ is interpreted as a scalar measure field of the concentration of imperfections.

We further postulate the evolution equations for the first group of internal state variables α_1 in the form

$$\partial_t \underset{\sim}{E}_p(\cdot,t) = \hat{\underset{\sim}{G}}(\sigma_1(\cdot,t)),$$
$$\partial_t \varkappa(\cdot,t) = \mathrm{tr}\left[\hat{\underset{\sim}{K}}(\sigma_1(\cdot,t))\,\partial_t \underset{\sim}{E}_p(\cdot,t)\right], \qquad (4.7)$$

and for the second group α_2 which is represented by the imperfection parameter ξ we assume the diffusion evolution equation

$$\partial_t \xi(\cdot,t) = D_0\,\nabla^2 \xi(\cdot,t) + \mathrm{tr}\left[\hat{\underset{\sim}{\Xi}}_1(\sigma_1(\cdot,t))\,\partial_t \underset{\sim}{E}_p(\cdot,t)\right]$$
$$+\ \hat{\Xi}_2(\sigma_1(\cdot,t)), \qquad (4.8)$$

where $\hat{\underset{\sim}{G}}$, $\hat{\underset{\sim}{K}}$, $\hat{\underset{\sim}{\Xi}}_1$ and $\hat{\Xi}_2$ are the material functions and D_0 denotes the diffusion constant.

4.2. Rate type material structure. Let us introduce the intrinsic state in the form as follows

$$\sigma_2(\cdot,t) = (\underset{\sim}{E}(\cdot,t),\ \underset{\sim}{T}(\cdot,t), \varkappa(\cdot,t), \xi(\cdot,t)). \qquad (4.9)$$

If we assume additionally that the constitutive equation (4.2) is such that $\underset{\sim}{E}_p(\cdot,t)$ can be expressed as function of $\underset{\sim}{E}(\cdot,t)$, $\underset{\sim}{T}(\cdot,t)$ and $\varkappa(\cdot,t)$ for any time $t \in [0,d_p]$, i.e.

$$\underset{\sim}{E}_p(\cdot,t) = \underset{\sim}{\hat{N}}(\underset{\sim}{E}(\cdot,t),\ \underset{\sim}{T}(\cdot,t), \varkappa(\cdot,t)) \qquad (4.10)$$

then the intrinsic state σ_2 can be obtained from σ_1 by taking advantage of Eq. (4.10).

Basing on the constitutive equation (4.2) we can write

$$\partial_t \underset{\sim}{T}(\cdot,t) = \partial_{\underset{\sim}{E}} \underset{\sim}{\hat{T}} \left[\partial_t \underset{\sim}{E}(\cdot,t)\right] + \partial_{\underset{\sim}{E}_p} \underset{\sim}{\hat{T}} \left[\partial_t \underset{\sim}{E}_p(\cdot,t)\right] + \partial_\varkappa \hat{T}\, \partial_t \varkappa(\cdot,t). \qquad (4.11)$$

The last result yields the evolution equation for the stress tensor $\underset{\sim}{T}(\cdot,t)$ as follows

$$\partial_t \underset{\sim}{T}(\cdot,t) = \underset{\sqcup}{\beta}_1 \left[\partial_t \underset{\sim}{E}(\cdot,t)\right] + \underset{\sim}{\beta}_0 \qquad (4.12)$$

where

$$\underset{\sqcup}{\beta}_1 = \partial_{\underset{\sim}{E}} \underset{\sim}{\hat{T}},$$

$$\underset{\sim}{\beta}_0 = \partial_{\underset{\sim}{E}_p} \underset{\sim}{\hat{T}} \left[\underset{\sim}{\hat{G}}(\sigma_2(\cdot,t))\right] + \partial_\varkappa \underset{\sim}{\hat{T}}\ \mathrm{tr}\left[\underset{\sim}{\hat{K}}(\sigma_2(\cdot,t))\ \underset{\sim}{\hat{G}}(\sigma_2(\cdot,t))\right], \qquad (4.13)$$

and additionally we have the evolution equation for ξ in the form

$$\partial_t \xi(\cdot,t) = D_0 \nabla^2 \xi(\cdot,t) + \mathrm{tr}\left[\underset{\sim}{\hat{\Xi}}_1(\sigma_2(\cdot,t))\ \partial_t \underset{\sim}{E}_p(\cdot,t)\right] + \underset{\sqcup}{\hat{\Xi}}_2(\sigma_2(\cdot,t)), \qquad (4.14)$$

6/ The conditions under which the internal state variable structure is isomorphic with the rate type material structure have been investigated in Ref. [32].

It is noteworthy that the evolution equation for the stress tensor (4.12) is not explicitly influenced by the rate $\dot{\xi}$ of the imperfection parameter ξ. This is consequence of the thermodynamic restriction superposed on the stress constitutive function $\hat{\tilde{T}}$.

5. Description of imperfections

5.1. Physical and experimental motivations. In the constitutive modelling for the postcritical behaviour we have to take into consideration the internal imperfections generated by the nucleation and growth of voids. As it has been pointed out by LE ROY, EMBURY, EDWARD and ASHBY [25] ductile fracture is the end of a sequence of three processes: (i) Nucleation of voids at second phase particles; (ii) Growth of voids mostly due to plastic deformation and yield stress state and due to the diffusional accommodated flow; (iii) Linkage of voids. It is assumed that voids coalesce when the void length reaches some multiple of its distance from the neighbouring void (cf. Figs. 1 and 2).

The most important experimental investigations of the failure of metals are those under the unidirectional tensile mode of loading. It can be expected that in the temperature - strain rate spectrum (cf. data of WRAY [51]) or in the temperature-flow stress spectrum (cf. Refs. [33,34]) different failure modes may occur. This conjecture is justified by the fact that different mechanisms of plastic flow should lead to different failure modes. We can say that these failure modes are the result of different fracture mechanisms.

From the fracture maps[7/] for 304 stainless steel (cf. Figs. 3 and 4) and for 316 stainless steel (cf. Figs. 5 and 6) it can be observed that most important fracture mechanisms are those of ductile fracture at low temperature, transgranular creep fracture and intergranular creep-controlled fracture as well as the pure diffusional fracture. The latter mechanism is not detected on the maps.

7/ A thorough investigation of the fracture maps for different materials can be found in Refs. [5,6,11,15].

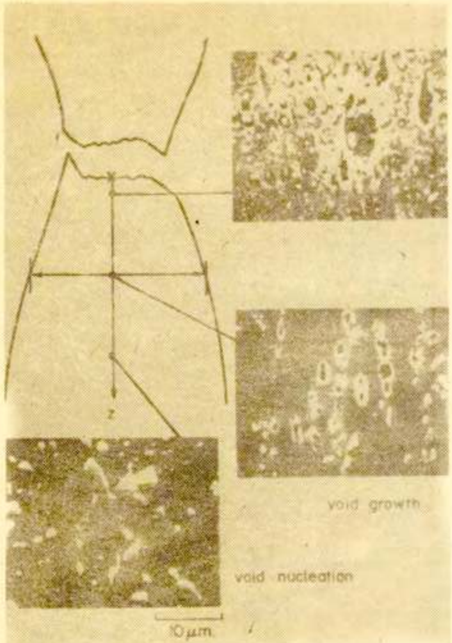

Fig.1

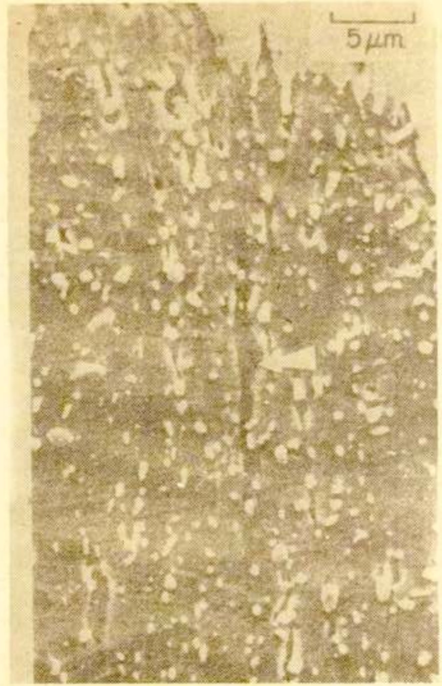

Fig.2

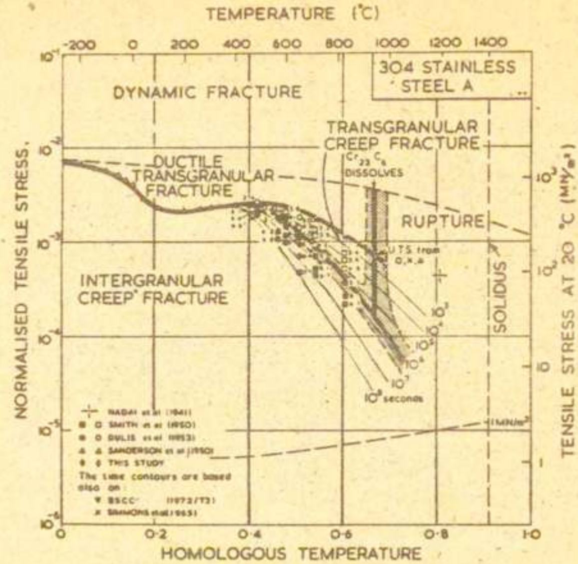

TEMPERATURE (°C)
304 STAINLESS STEEL A
DYNAMIC FRACTURE
TRANSGRANULAR CREEP FRACTURE
DUCTILE TRANSGRANULAR FRACTURE
RUPTURE
INTERGRANULAR CREEP FRACTURE
SOLIDUS
NORMALISED TENSILE STRESS,
TENSILE STRESS AT 20 °C (MN/m²)
HOMOLOGOUS TEMPERATURE

Fig.3

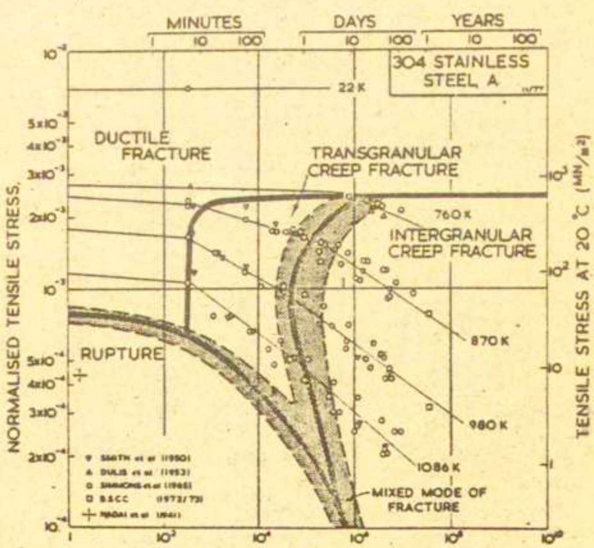

MINUTES
DAYS
YEARS
304 STAINLESS STEEL A
22 K
DUCTILE FRACTURE
TRANSGRANULAR CREEP FRACTURE
760 K
INTERGRANULAR CREEP FRACTURE
870 K
RUPTURE
980 K
1086 K
MIXED MODE OF FRACTURE
NORMALISED TENSILE STRESS,
TENSILE STRESS AT 20 °C (MN/m²)
FAILURE TIME (seconds)

Fig.4

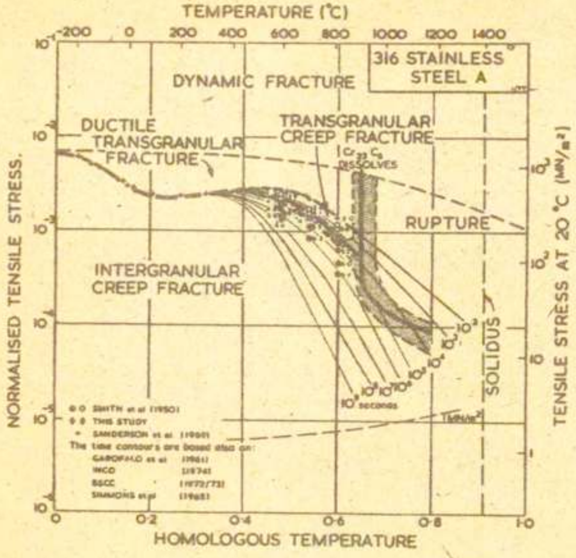
TEMPERATURE (°C)
316 STAINLESS STEEL A
DYNAMIC FRACTURE
DUCTILE TRANSGRANULAR FRACTURE
TRANSGRANULAR CREEP FRACTURE
RUPTURE
INTERGRANULAR CREEP FRACTURE
SOLIDUS
NORMALISED TENSILE STRESS.
TENSILE STRESS AT 20 °C (MN/m²)
HOMOLOGOUS TEMPERATURE

Fig.5

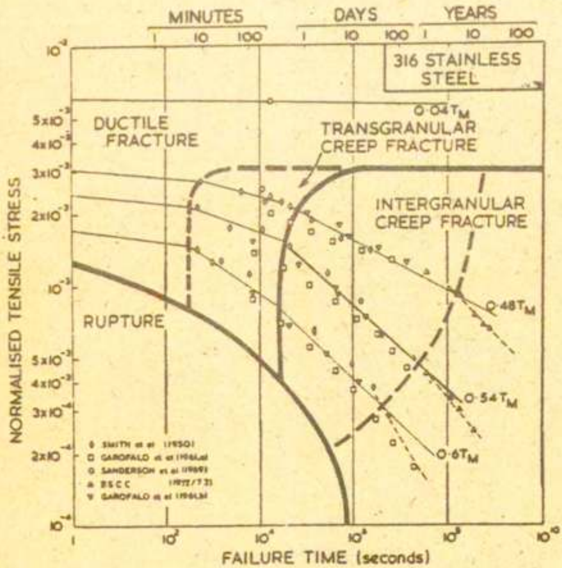
MINUTES
DAYS
YEARS
316 STAINLESS STEEL
DUCTILE FRACTURE
TRANSGRANULAR CREEP FRACTURE
INTERGRANULAR CREEP FRACTURE
RUPTURE
0·48T_M
0·54T_M
0·6T_M
NORMALISED TENSILE STRESS
FAILURE TIME (seconds)

Fig.6

We shall concentrate our attention on these four flow and fracture mechanisms.

To collect most important features for all of these fracture mechanism it would be useful to discuss physical nature of every mechanism separatly.

Polycrystalline solids, when they do not cleave, may fail in a ductile, transgranular way. Voids or holes nucleate at inclusions, further plasticity of a material makes them grow and when they are large enough or when the specimen during tensile test itself becomes mechanically unstable, they coalesce and the material fracture.

At temperature above 0.3 ϑ_M metals creep. The flow stress depends on strain rate and the thermo-activated process for dislocation creep occurs. Voids or holes nucleate at inclusions within the grains and grow as the material creep, until they coalesce to give a fracture path. This mechanism is called the transgranular creep fracture.

At lower stresses, and longer times-to-fracture, a transition from transgranular to an intergranular fracture is observed. Within this new regime, grain boundaries slide, wedge-cracks or voids grow on boundaries lying roughly normal to the tensile axis. Fracture is directly controlled by thermally-activated dislocation creep and often may be approximated by the power-law creep. The shapes of the grain-boundary voids or cracks suggest that the diffusion-accommodated flow process contributes to their growth.

When the temperature is high enough to permit diffusion process, and stress so low that creep process is negligible voids or holes on grain boundaries in stressed solids can grow by pure diffusion mechanism.

From this consideration it is clear that the postcritical behaviour of ductile solids is controlled by several cooperative mechanisms. We can recognize some characteristic features for all of them.

First, the most essential are the nucleation and growth of voids. The behaviour of the bulk specimen in tensile test is influenced by evolution of voids during the deformation process.

Second, temperature and strain rate sensitivity of the material is also observed as very important. It means that for regions in which these mechanisms operate the thermally-activated process for very low strain rate can be assumed as responsible for dislocation creep flow.

Third, for intergranular creep-controlled flow and for pure diffusional mechanism the transport phenomena contribute to void growth. The transport process is usually approximated by the diffusion cooperative mechanism.

LE ROY, EMBURY, EDWARD and ASHBY[25] have shown that voids nucleated both by the cracking of carbides and by their decohesion 8/. Once nucleated, the voids grow mainly in the tensile dirertion and only in the late stages of necking. When the triaaxiality is large does tranverse growth occur. As all the voids did not nucleate at the same strain, a certain range of void sizes can be observed at a given strain level. When decohesion occurs on one side of the particle only, the free end of the void grows in the longitudinal direction until it meets another particle, forming a long and narrow cavity or a vertical chain of cavities as decohesion latter occurs at the other side of the particle also.

The number of voids and their area fraction are shown, as a function of strain in Figs. 7 and 8. The volume fraction of boids increases slowly at first, approximately linearly with strain, until a threshold value is reached, beyond which it increases rapidly.

8/ Cf. here also suggestions presented by GURLAND [16] and investigations conducted by FISHER [13]. Fisher noted that a better understanding of the mechanics of ductile fracture requires further study of the micromechanisms which operate during the early stages of void initiation. Current fracture models attempt to relate microstructure to the critical conditions for crack initiation and growth and help to characterize the fracture process in engineering materials. In void nucleation processes very instrumental are particles and inclusions (inhomogeneities in polycrystalline materials). Particle fracture and interfacial decohesion result as a consequence of the local state of deformation which exists in the vicinity of void inhomogeneities. Existing models for void nucleation are generally grouped into one of three categories based upon either an energy criterion, a local stress criterion or a local strain criterion is postulated.

Fracture occurs by the transverse linking of the elongated voids in plane which is macroscopically normal to the tensile axis. Very few connected voids are observed below the fracture surface, which illustrates the highly localized and catastrophic character of the final coalescence process.

The conditions for the void coalescence are not well understood, although some authors show the influence of strain rate sensitivity and the effect of partial adhesion of the particle and matrix as most important factors.

In a model based on continuous nucleation of voids LE ROY, EMBURY, EDWARD and ASHBY [25] assume that the number of cracked particles increases linearly with strain. This assumption is in agreement with the initial portion of the curves shown in Figs. 7 and 8.

Basing on careful examination of the void nucleation, the void growth and the accumulation of damage during tensile loading and the subsequent necking process and taking advantage of physical suggestions we can assume proper evolution equation for the scalar measure of the concentration of imperfections ξ.

It is worth to note that in many recent investigations the analysis of the growth of cavities along grain interfaces by the combined processes of grain boundary diffusion and plastic dislocation creep in the adjoining grains has been given. However, this model[9/] is based on the assumption that coupling between the processes can be expressed in terms of a parameter L, which has the dimensions of length and which is a function of material properties, temperature and applied stress /cf. RICE [44], NEEDLEMAN and RICE [30] and SHAM and NEEDLEMAN [46]/. This idea describes the coupling in situations when extensive dislocation creep allows local accommodation of matter diffused into the grain boundary from the cavity walls but it is not in the position to describe the boundary-spatial effect observed for the bulk specimen in tensile test.

9/ Physical foundations for this model were presented by HULL and RIMMER [23], SPEIGHT and HARRIS [47] and WEERTMAN [49,50], cf. also HERRING [18] and COBLE [10].

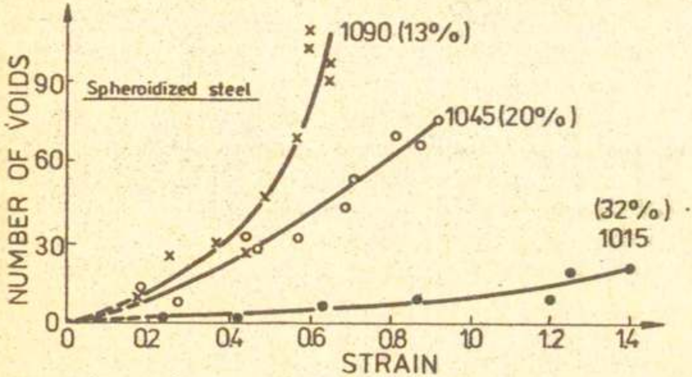
NUMBER OF VOIDS
Spheroidized steel
1090 (13%)
1045 (20%)
(32%)
1015
0
30
60
90
0
0.2
0.4
0.6
0.8
1.0
1.2
1.4
STRAIN

Fig.7

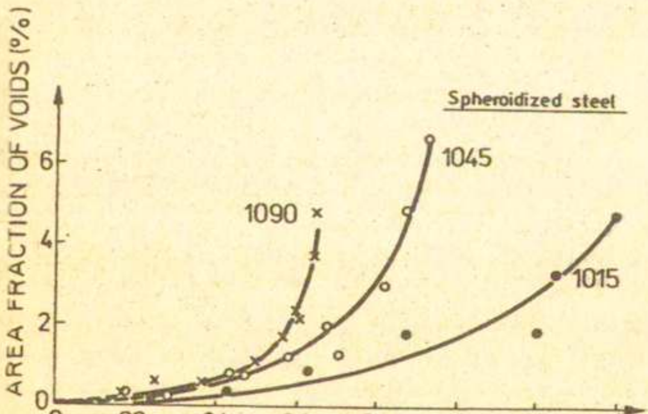
AREA FRACTION OF VOIDS (%)
Spheroidized steel
1045
1090
1015
0
2
4
6
0
0.2
0.4
0.6
0.8
1.0
1.2
1.4
STRAIN

Fig.8

5.2. Theoretical proposition. Our aim is to describe the evolution of imperfections generated by the nucleation and growth of voids and to take into consideration the transport phenomena suggested by the physical mechanisms. To do this we postulate the evolution equation for the imperfection parameter ξ in the form

$$\partial_t \xi = (\partial_t \xi)_{diffusion} + (\partial_t \xi)_{nucleation} + (\partial_t \xi)_{growth} \cdot \quad (5.1)$$

The comparison of the postulated evolution equation (4.8) with (5.1) gives

$$(\partial_t \xi)_{diffusion} = D_o \nabla^2 \xi (x,t) \quad (5.2)$$

and

$$(\partial_t \xi)_{nucleation} + (\partial_t \xi)_{growth} = tr(\hat{\underset{\sim}{\Xi}}_1 \, \partial_t \underset{\sim}{E}_p) + \hat{\Xi}_2 , \quad (5.3)$$

where D_o is the diffusion constant properly assumed for particular material, $\hat{\underset{\sim}{\Xi}}_1$ and $\hat{\Xi}_2$ are two material functions which have to be determined.

To fix precisely the diffusion constant D_o we can use the expression

$$D(\vartheta) = const \quad exp\left(-\frac{U_D}{R\vartheta}\right) , \quad (5.4)$$

where U_D is the activation energy of the diffusion process assumed, R denotes the gas constant and ϑ temperature. By proper selection of the diffusion process[10/] we can determine the activation energy U_D as a function of temperature. For isothermal process, that is for constant temperature we can assume

$$D_o = D(\vartheta) \Big|_{\vartheta = \vartheta_o} \quad (5.5)$$

To determine the material functions $\hat{\underset{\sim}{\Xi}}_1$ and $\hat{\Xi}_2$ we take advantage of previously discussed physical and experimental motivations.

Experimental result suggest that growth $(\partial_t \xi)$ in the first approximation can be assumed as proportional to the inelastic strain rate. On the other hand physical consideration imply that nucleation $(\partial_t \xi)$ is connected with the inelastic power and with

---

10/ For a thorough discussion of diffusion processes in solids see FLYNN [12].

the rate of the first invariant of the stress tensor.

Basing on these suggestions we postulate

$$\hat{\underset{\sim}{\Xi}}_1 = (m - \xi)\, \underset{\sim}{\Xi}_0 + \frac{h}{m-\xi}\, \underset{\sim}{T}\,,$$
$$\hat{\Xi}_2 = l\, j_1\,, \qquad (5.6)$$

where m is interpreted as a limit value for ξ , $\underset{\sim}{\Xi}_0$ denotes the material constant matrix, h is the material function and l denotes the material constant.

As a consequence of the postulates assumed we have the evolution equation for the imperfection parameter ξ in the form as follows

$$\partial_t \xi(X,t) = D_0 \nabla^2 \xi(X,t) + (m-\xi)\,\mathrm{tr}(\underset{\sim}{\Xi}_0 \partial_t \underset{\sim}{E}_p) + \frac{h}{m-\xi}\,\mathrm{tr}(\underset{\sim}{T}\, \partial_t \underset{\sim}{E}_p) + l\, j_1\,. \qquad (5.7)$$

6. Elastic-viscoplastic solids with internal imperfections.

6.1. Internal state variable description. To describe the elastic-viscoplastic response of a material we have to specify the evolution equation for the inelastic strain tensor $\underset{\sim}{E}_p$. It means to specify the function $\hat{\underset{\sim}{G}}$ in the evolution equation (4.7). Let us postulate (cf. Refs. [33-35])

$$\hat{\underset{\sim}{G}}(\sigma) = \frac{\gamma}{\varphi}\left\langle \Phi\left(\frac{f(\cdot)}{\varkappa} - 1\right)\right\rangle \partial_{\underset{\sim}{T}} f(\cdot)\,, \qquad (6.1)$$

where γ_0 is the viscosity constant, φ is interpreted as the control function and is assumed to depend on $\frac{I_2}{I_2^s} - 1$, $I_2 = (II_{\dot{E}})^{1/2}$ is the second invariant of the strain rate tensor, $I_2^s = (\widetilde{II}_{\dot{E}_s})^{1/2}$ and $\underset{\sim}{E}_s$ is the static strain rate tensor, Φ denotes the overstress viscoplastic function, $f(\cdot)$ is the quasi-static yield function and is postulated as

$$f(\cdot) = f(\underset{\sim}{T}, E_p, \xi) \qquad (6.2)$$

the symbol $\langle[\ ]\rangle$ is understood according to the definition

$$\langle[\ ]\rangle = \begin{cases} 0 & \text{if} \quad f(\cdot) \leqslant \varkappa \, , \\ [\ ] & \text{if} \quad f(\cdot) > \varkappa \, . \end{cases} \tag{6.3}$$

For the control function φ we postulate (cf. Ref. [34])

$$\lim_{I_2 = I_2^s} \varphi = 0 \quad \text{and} \quad \varphi(\cdot) = 0 \text{ for } I_2 < I_2^s \, . \tag{6.4}$$

The elastic-viscoplastic response of a material is determined by the constitutive equation for the Piola-Kirchhoff stress tensor (cf. Eq. (4.2))

$$\underset{\sim}{T} = \hat{\underset{\sim}{T}}(\underset{\sim}{E}, \underset{\sim}{E}_p, \varkappa) \tag{6.5}$$

and the evolution equations for the internal state variables $\underset{\sim}{E}_p$, $\varkappa$ and ξ postulated in the form as follows

$$\begin{aligned} \partial_t \underset{\sim}{E}_p(X,t) &= \frac{\gamma_0}{\varphi} \left\langle \Phi\left(\frac{f(\cdot)}{\varkappa} - 1 \right) \right\rangle \partial_{\underset{\sim}{T}} f(\cdot) \, , \\ \partial_t \varkappa(X,t) &= \mathrm{tr}\left[\hat{\underset{\sim}{K}}(\sigma) \partial_t \underset{\sim}{E}_p(X,t) \right] , \\ \partial_t \xi(X,t) &= D_0 \nabla^2 \xi(X,t) + (m - \overset{*}{\xi}) \mathrm{tr}\left[\underset{\sim}{\Xi}_0 \partial_t \underset{\sim}{E}_p(X,t) \right] \\ &\quad + \frac{h}{m - \xi} \mathrm{tr}\left[\underset{\sim}{T} \partial_t \underset{\sim}{E}_p(X,t) \right] + l j_1 \, . \end{aligned} \tag{6.6}$$

The evolution equations postulated have some important features[11/]. First, by introducing the control function φ the

---

11/ For physical motivations of the elastic-viscoplastic model with internal imperfections see Ref. [36]. It has been shown (cf. ASHBY and VERRALL [7]) that when strain rate is small (10^{-8} - $10^{-4} s^{-1}$) and the temperature is high enough to permit diffusion and when strain are large (as in superplastic flow), the flow process can be modelled by a grain-boundary sliding mechanism with diffusional accommodation. For higher strain rates (10^{-4} - 10^{-2} s^{-1}) dislocation creep flow is more dominant. The elastic-viscoplastic model with internal imperfections is based on the assumption that each void when nucleated grows by inelastic deformation and by diffusion, but the void plus its diffusiomodel proposed can describe the properties of material in a range of strain rates near the static value $I_2 = I_2^s$. This model satisfies also the requirement that during the deformation process in which the effective strain rate is equal to the static value the response of a material becomes elastic-plastic. Second, it can describe the evolution of imperfections during the deformation process by taking account of the nucleation of voids as well as the growth of voids. Third, it includs in the description the diffusional accommodated flow process.

To describe the evolution of the intrinsic state for a body B we need the initial values

$$\begin{aligned} \underset{\sim}{E}_p(X,0) &= \underset{\sim}{E}_p^o(X), \\ \varkappa(X,0) &= \varkappa^o(X), \\ \xi(X,0) &= \xi^o(X), \end{aligned} \qquad (6.7)$$

for $t = 0$ and for $X \in B$, and the boundary condition for the imperfection parameter ξ in the form

$$a\partial_{\underset{\sim}{n}}\xi(X,t) + b\,\xi(X,t) = 0 \qquad (6.8)$$

for $(X,t) \in (\partial B \times [0, d_p])$, where a and b are constant values.

6.2. Rate type material structure in Eulerian description.

We shall nowe use different method than that proposed in Section 4.2 to formulate the equations which describe the elastic-viscoplastic response in the form of the rate type material structure.

Let us denote the symmetric rate of deformation tensor by $\underset{\sim}{D}$ and postulate

$$\begin{aligned} \underset{\sim}{D}^e &= \underset{\sim}{D} - \underset{\sim}{D}^p, \\ \underset{\sim}{D}^e &= \frac{1}{2G}\left[\overset{\nabla}{\underset{\sim}{\sigma}} - \frac{\nu}{1+\nu}\, \mathrm{tr}\,\overset{\nabla}{\underset{\sim}{\sigma}}\, I\right], \\ \underset{\sim}{D}^p &= \frac{\gamma_0}{\varphi\left(\frac{I_2}{I_2^s}-1\right)}\left\langle \Phi\left[\frac{f(J_1, J_2', J_3', \xi)}{\varkappa} - 1\right]\right\rangle \partial_{\underset{\sim}{\sigma}} f(\cdot), \end{aligned} \qquad (6.9)$$

---

nal field is contained within a cell of a thermo-activated flowing material.

Cf. also the physical consideration presented by PĘCHERSKI [40,41] in which the modified evolution equation in the form $(6.6)_4$ is justified.

where $\overset{\nabla}{\sigma}$ denotes the symmetric Zaremba-Jaumann rate of change of the Cauchy stress tensor σ, G is the shear modulus and ν is the Poison ratio, by J_1 we denote the first invariant of the Cauchy stress tensor σ and J_2' and J_3' are used to denote the second and third invariants of the stress deviator, respectively.

As the result of Eqs. (6.9) we have the evolution equation for the Cauchy stress tensor σ in the form

$$\frac{1}{2G}\left[\overset{\nabla}{\sigma} - \frac{\nu}{1+\nu}\, t_r \overset{\nabla}{\sigma}\, I\right] = D - \frac{\gamma_0}{\varphi\left(\frac{I_4}{I_2^5}-1\right)}\left\langle \phi\left[\frac{f(J_1, J_2', J_3', \xi)}{\varkappa} - 1\right]\right\rangle \partial_{\sigma} f(\cdot)\,. \tag{6.10}$$

The intrinsic state σ is now assumed in the form

$$\sigma = (e, \sigma, \varkappa, \xi)\quad , \tag{6.11}$$

where e denotes the Cauchy strain tensor.

We need additionally the evolution equations for the internal state variables $\varkappa$ and ξ . Let us first focus on the imperfection parameter ξ .

To compare the scalar measure of the concentration of imperfections ξ with the void volume fraction parameter introduced by GURSON [17], cf. also NEEDLEMAN and RICE [29] and SAJE, PAN and NEEDLEMAN [45] we have to consider the voided solids (porous solids) . For this new interpretation of the imperfection parameter ξ we have to assume m=1 . We shall denote by $\bar{\sigma}$ the tensile flow strength of the matrix material, $\bar{\varepsilon}_p$ the matrix equivalent plastic tensile strain and $h = d\sigma / d\bar{\varepsilon}^p$ the equivalent tensile hardening rate of the matrix material.

Equivalence of plastic work (cf. Refs. [29,45,48])

$$(1-\xi)\,\bar{\sigma}\,\dot{\bar{\varepsilon}}^p = tr\,(\sigma D^p) \tag{6.12}$$

gives

$$\dot{\bar{\sigma}} = \frac{\bar{h}}{(1-\xi)\,\bar{\sigma}}\; tr\,(\sigma D^p) \tag{6.13}$$

If we assume after NEEDLEMAN and RICE [29] and SAJE, PAN and NEEDLEMAN [45]

$$(\dot{\xi})_{nucleation} = A\,\dot{\bar{\sigma}} + B\,\dot{J}_1 \tag{6.14}$$

and take advantage of (6.13) we have

$$(\dot{\xi})_{nucleation} = \frac{h}{1-\xi} \operatorname{tr}(\underset{\sim}{\sigma} \underset{\sim}{D} \quad + l j_1 \ , \qquad (6.15)$$

where

$$h = \frac{A \bar{h}}{\bar{\sigma}} \qquad (6.16)$$

as has been postulated by Eq. $(5.6)_1$ The result (6.16) gives new interpretation for the material function h.

If we keep postulates (5.2) and (5.3) i.e.

$$(\dot{\xi})_{growth} = (1-\xi) \operatorname{tr}(\underset{\sim}{\Xi}_o \underset{\sim}{D}^p) , \qquad (6.17)$$

$$(\dot{\xi})_{diffusion} = D_o \nabla^2 \xi$$

we can write the evolution equation for the void volume fraction ξ in the form as follows

$$\dot{\xi} = D_o \nabla^2 \xi + \frac{h}{1-\xi} \operatorname{tr}(\underset{\sim}{\sigma} \underset{\sim}{D}^p) + l j_1 + (1-\xi) \operatorname{tr}(\underset{\sim}{\Xi}_o \underset{\sim}{D}^p) \qquad (6.18)$$

We shall consider the following yield functions for voided material (cf. Refs. [29,45,48])

(i) $f(\cdot) = (J_2')^{1/2}$ and $\varkappa = \varkappa_o (1-\xi^{1/2})$,

(ii) $f(\cdot) = J_2' (1 + n\xi \frac{J_1^2}{J_2'})$ and $\varkappa = \varkappa_o^2 (1-\xi^{1/2})$, (6.19)

(iii) $f(\cdot) = J_2' (1 - 0.73 \frac{J_3'^2}{J_2'^3} + n\xi \frac{J_1^2}{J_2'})$ and $\varkappa = \varkappa_o^2 (1-\xi^{1/2})$,

(iv) $f(\cdot) = 3J_2' + 2\xi \bar{\sigma}^2 \cosh(\frac{3J_1}{2\bar{\sigma}})$ and $\varkappa = \bar{\sigma}^2 (1+\xi^2)$,

(v) $f(\cdot) = 3J_2' + 2\xi \bar{\sigma}^2 n_1 \cosh(\frac{3n_2 J_1}{2\bar{\sigma}})$ and $\varkappa = \bar{\sigma}^2 (1+n_3 \xi^2)$.

The work hardening parameter $\varkappa$ is now assumed to play a role of the material function which is postulated in the particular form for every case considered.

We shall write down the evolution equation for the inelastic deformation for two first examples of the yield function.

We have the following results

(i) $$\underset{\sim}{D}^{p} = \frac{\gamma_o}{\varphi\left(\frac{I_2}{I_2^s}-1\right)} \left\langle \Phi\left[\frac{\sqrt{J_2'}}{\varkappa_o(1-\xi^{1/2})}-1\right]\right\rangle \frac{\underset{\sim}{S}}{\sqrt{J_2'}} \qquad (6.20)$$

(ii) $$\underset{\sim}{D}^{p} = \frac{\gamma_o}{\varphi\left(\frac{I_2}{I_2^s}-1\right)} \left\langle \Phi\left[\frac{J_2'+n\xi J_1^2}{\varkappa_o^2(1-\xi^{1/2})}-1\right]\right\rangle \frac{\underset{\sim}{S}+2n\xi J_1\underset{\sim}{I}}{\varkappa_o}.$$

It is noteworthy that even in the case when we assume the material function the workhardening effect of a material can be included into consideration by interpreting as isotropic work hardening parameter. In this point we shall be flexible.

7. Elastic-plastic response

The elastic-plastic response of a material is reached in the limit case, when $I_2 = I_2^s$. Then we have the evolution equations as follows

$$\underset{\sim}{D}^{p} = \Lambda \partial_{\underset{\sim}{\sigma}} f(\cdot)$$

$$\dot{\xi} = \frac{8\,\bar{h}}{1-\xi}\,\mathrm{tr}(\underset{\sim}{\sigma}\underset{\sim}{D}^{p}) + (j_1 + (1-\xi)\,\mathrm{tr}(\underset{\sim}{\Xi}_o \underset{\sim}{D}^{p}) \qquad (7.1)$$

for

$$f(\cdot) = \varkappa \quad \text{and} \quad \mathrm{tr}(\partial_{\underset{\sim}{\sigma}} f\,\dot{\underset{\sim}{\sigma}}) > 0 \qquad (7.2)$$

It is noteworthy that the diffusion effect has been neglected. The parameter Λ can be determined from the condition

$$\dot{f} = \dot{\varkappa} \qquad (7.3)$$

The evolution equation for the plastic deformation in index notation can be written in the form (cf. Refs. [29,45])

$$D^{p}_{ij} = \frac{1}{H} P_{ij} Q_{kl} \overset{\nabla}{\sigma}_{kl}, \qquad (7.4)$$

where

$$P_{ij} = \frac{\partial f}{\partial \sigma_{ij}}, \quad Q_{kl} = \frac{\partial f}{\partial \sigma_{kl}} + \frac{1}{3}\frac{\partial f}{\partial \xi}\,l\,\delta_{kl}, \qquad (7.5)$$

$$H = -\left[(1-\xi)\frac{\partial f}{\partial \xi}\,\delta_{ij}\frac{\partial f}{\partial \sigma_{ij}} + \frac{\bar{h}}{(1-\xi)\bar{\sigma}}\left(A\frac{\partial f}{\partial \xi} + \frac{\partial f}{\partial \bar{\sigma}}\right)\sigma_{ij}\frac{\partial f}{\partial \sigma_{ij}}\right].$$

As examples let us consider the two yield functions (cf.(6.19))

For the first case

(i) $$f(\cdot) = (J_2')^{1/2} \text{ and } \varkappa = \hat{\varkappa}(\xi) = \varkappa_0(1-\xi^{1/2}), \quad \xi \in [0,1], \tag{7.6}$$

we have

$$\begin{aligned} \partial_{\sigma} f &= \underset{\sim}{S} (J_2')^{1/2}, \\ D^p_{ij} &= \frac{1}{H} \frac{S_{ij}}{\sqrt{J_2'}} \frac{S_{kl}}{\sqrt{J_2'}} \overset{\nabla}{\sigma}_{kl}, \\ D^p_{ij} &= \frac{1}{H} P_{ij} Q_{kl} \overset{\nabla}{\sigma}_{kl}, \end{aligned} \tag{7.7}$$

where

$$P_{ij} = \frac{S_{ij}}{2\tau_e}, \quad Q_{kl} = \frac{S_{kl}}{2\tau_e}, \quad \tau_e = \sqrt{J_2'}$$

$$H = 4 \frac{\partial \hat{\varkappa}}{\partial \xi} \sqrt{J_2'} \left[\frac{1-\xi}{J_2'} \Xi^0_{ij} S_{ij} + \frac{2h}{1-\xi} \right], \tag{7.8}$$

$$S_{ij} = \sigma_{ij} - \frac{1}{3} (\sigma_{kk}) \delta_{ij}.$$

For the second case

(ii) $$f(\cdot) = J_2'\left(1 + n\xi \frac{J_1^2}{J_2'}\right) \text{ and } \varkappa = \hat{\varkappa}(\xi) = \varkappa_0^2 (1-\xi^{1/2}), \tag{7.9}$$

then

$$P_{ij} = \frac{S_{ij}}{2\tau_e} + \frac{\beta}{3} \delta_{ij}, \quad Q_{kl} = \frac{S_{kl}}{2\tau_e} + \frac{\mu}{3} \delta_{kl}, \tag{7.10}$$

where

$$\begin{aligned} \beta &= \frac{3n\xi J_1}{\sqrt{\varkappa_0^2 (1-\xi^{1/2}) - n\xi J_1^2}}, \\ \mu &= \beta + \frac{\iota(nJ_1^2 + \frac{1}{2}\varkappa_0^2 \xi^{-1/2})}{2\sqrt{\varkappa_0^2(1-\xi^{1/2}) - n\xi J_1^2}}, \end{aligned} \tag{7.11}$$

$$H = -\frac{1}{4\tau_e^2} \left[(1-\xi) \Xi^0_{ij} \frac{\partial f}{\partial \sigma_{ij}} + \frac{h}{1-\xi} \sigma_{ij} \frac{\partial f}{\partial \sigma_{ij}} \right] \left(\frac{\partial f}{\partial \xi} - \frac{\partial \hat{\varkappa}}{\partial \xi} \right).$$

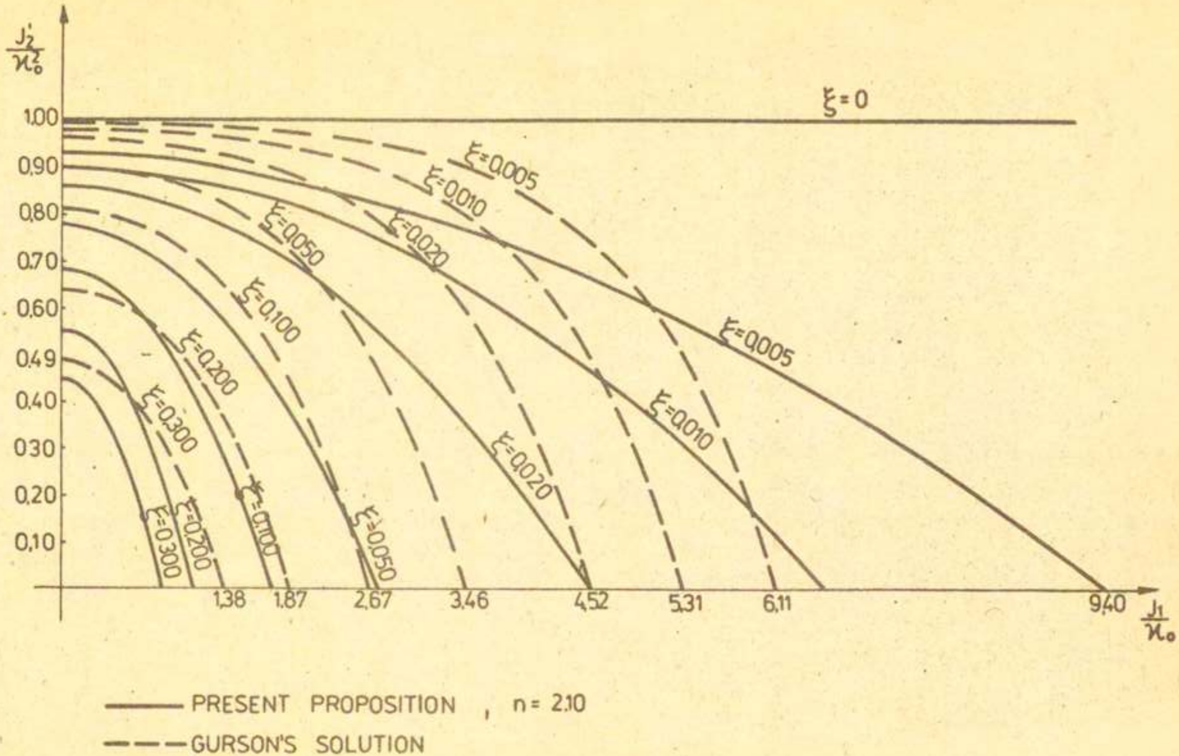

$J_2'/\varkappa_0^2$
1,00
0,90
0,80
0,70
0,60
0,49
0,40
0,30
0,20
0,10
$\xi = 0$
$\xi = 0{,}005$
$\xi = 0{,}010$
$\xi = 0{,}020$
$\xi = 0{,}050$
$\xi = 0{,}100$
$\xi = 0{,}200$
$\xi = 0{,}300$
$\xi = 0{,}005$
$\xi = 0{,}010$
$\xi = 0{,}020$
$\xi = 0{,}050$
$\xi = 0{,}100$
$\xi = 0{,}200$
$\xi = 0{,}300$
1,38
1,87
2,67
3,46
4,52
5,31
6,11
9,40
$J_1/\varkappa_0$
PRESENT PROPOSITION , n = 2.10
GURSON'S SOLUTION

Fig.9

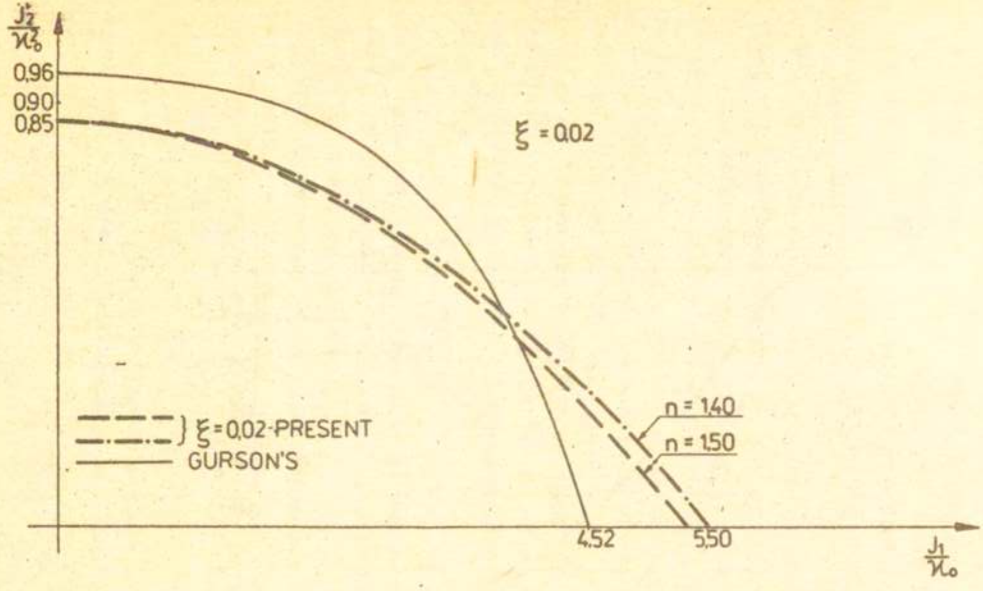

$\frac{J_2'}{\varkappa_0^2}$
0,96
0,90
0,85
ξ = 0,02
} ξ = 0,02-PRESENT
GURSON'S
n = 1,40
n = 1,50
4,52
5,50
$\frac{J_1}{\varkappa_0}$

Fig.10

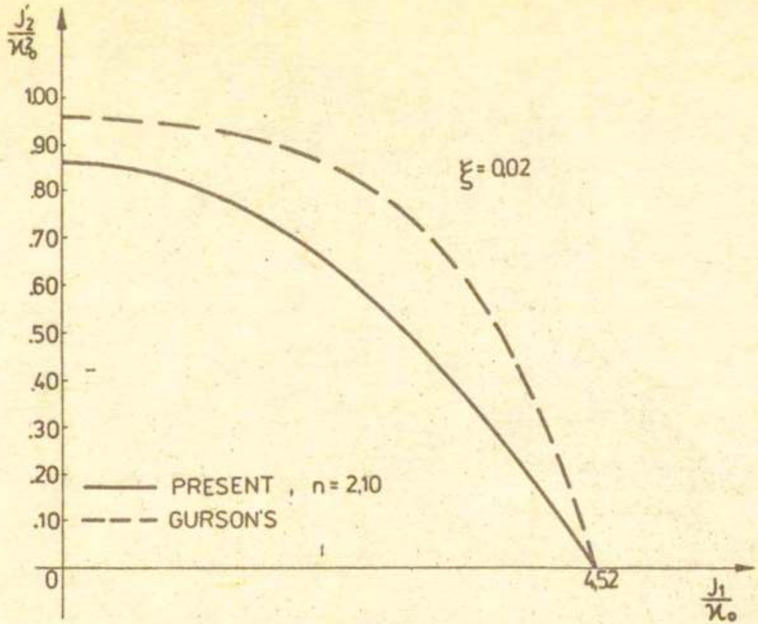
J'2/κ0²
1.00
.90
.80
.70
.60
.50
.40
.30
.20
.10
0
4.52
J1/κ0
ξ = 0.02
PRESENT , n = 2.10
GURSON'S

Fig.11

It is noteworthy that the normality does not apply because $\mu \neq \beta$. If $l = 0$ then $\mu = \beta$, $P_{ij} = Q_{ij}$ and normality applies.

The comparison of the Gurson solution (cf. Ref. [17]) with the present proposition is given in Fig. 9.

In Figs. 10 and 11 it has been shown the influence of the constant n on the results for $\xi = 0.02$.

8. Identification procedure

8.1. Basing on mechanical tests. To determine the material functions and constants involved in the evolution equation for the inelastic deformation tensor E_p we shall use the available experimental data obtained in dynamical tests. As it has been shown in Ref. [34] the determination of the material function Φ, the control function φ and the material constants can be based on both the combined as well one-dimensional loading tests.

We shall use the procedure of identification developed for the elastic-perfectly viscoplastic material in Ref. [34] and generalized to the elastic-work hardening viscoplastic material in Ref. [39].

Let us show this procedure first for the dynamical tests under combined loading. We shall use two experimental data obtained by LINDHOLM [26] for mild steel and by RANDALL and CAMPBELL [42] for a low-carbon steel.

From these works for particular metals we have the experimental curves as follows

$$(II_{\varepsilon})^{1/2} = \mathcal{G}(I_2)_{(II_{\varepsilon})^{1/2}} = \text{const} . \tag{8.1}$$

Using as an optimum criterion for the best fitting of experimental data by theoretical results the functional

$$\mathcal{J} = \max_{\substack{t \in [0, d_p] \\ I_2(t) \in (I_2^s, I_2^{max})}} \left\| J_2'(t) - \mathcal{G}(I_2) \Big|_{(II_{\varepsilon})^{1/2} = \text{const}} \right\| \tag{8.2}$$

where

$$J_2'(t) = \varkappa \left\{ 1 + \Phi^{-1}\left[\frac{(\mathrm{tr}(\dot{E}_p(t))^2)^{1/2}}{\gamma_0} \varphi\left(\frac{I_2}{I_2^s} - 1\right)\right]\right\} , \tag{8.3}$$

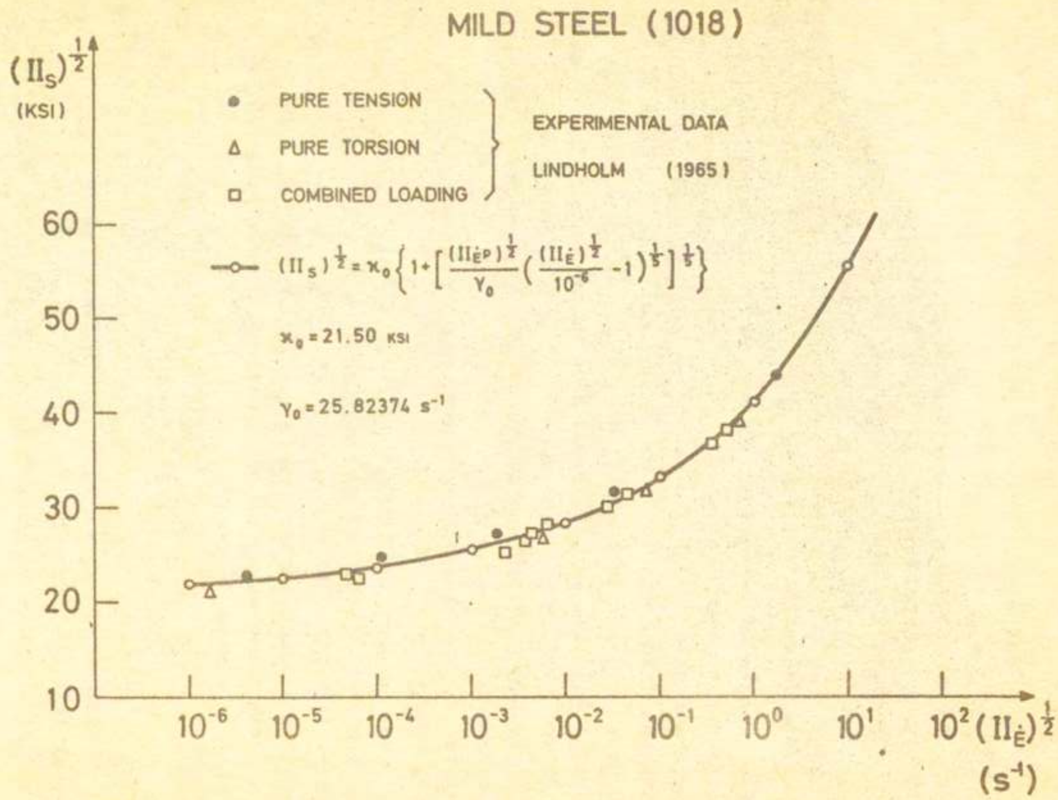
MILD STEEL (1018)
$(II_S)^{\frac{1}{2}}$
(KSI)
PURE TENSION
PURE TORSION
COMBINED LOADING
EXPERIMENTAL DATA
LINDHOLM (1965)
$(II_S)^{\frac{1}{2}} = \varkappa_0 \left\{ 1 + \left[\frac{(II_{\dot{E}^P})^{\frac{1}{2}}}{\gamma_0} \left(\frac{(II_{\dot{E}})^{\frac{1}{2}}}{10^{-6}} - 1 \right)^{\frac{1}{5}} \right]^{\frac{1}{5}} \right\}$
$\varkappa_0 = 21.50$ KSI
$\gamma_0 = 25.82374\ s^{-1}$
60
50
40
30
20
10
10^{-6}
10^{-5}
10^{-4}
10^{-3}
10^{-2}
10^{-1}
10^{0}
10^{1}
10^{2}
$(II_{\dot{E}})^{\frac{1}{2}}$
(s^{-1})

Fig.12

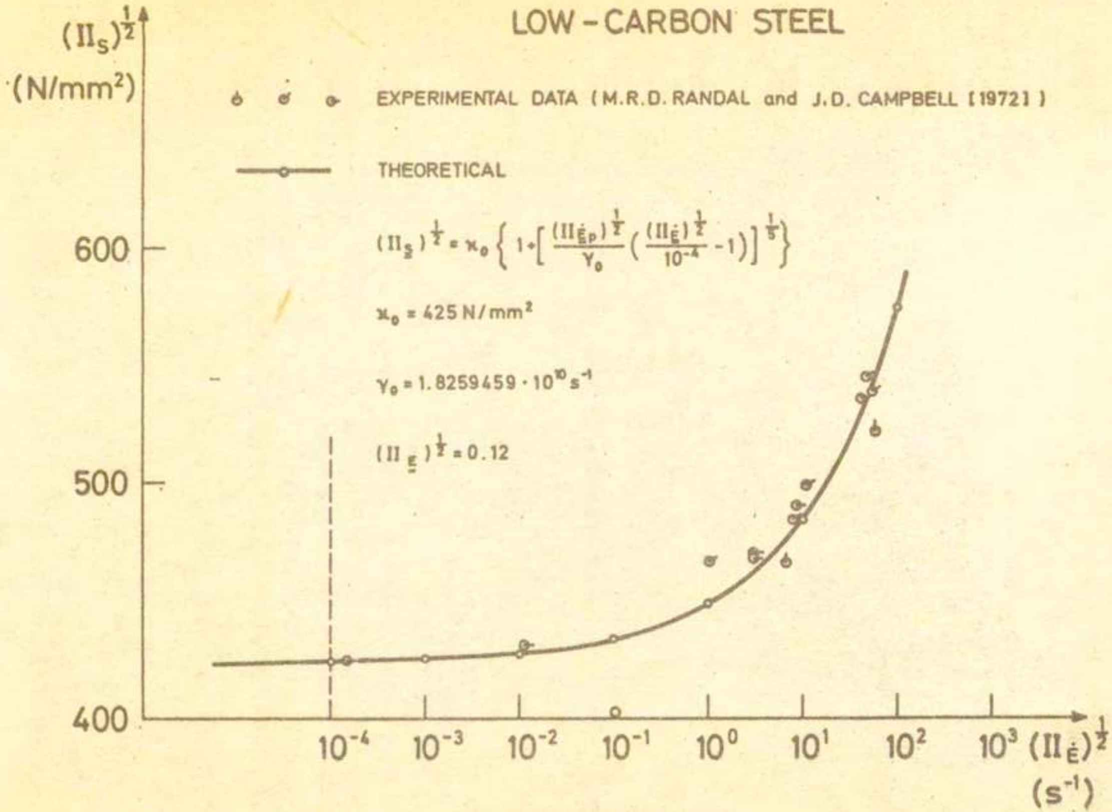

LOW - CARBON STEEL
$(II_S)^{\frac{1}{2}}$ (N/mm²)
EXPERIMENTAL DATA (M.R.D. RANDAL and J.D. CAMPBELL [1972])
THEORETICAL
$(II_S)^{\frac{1}{2}} = \varkappa_0 \left\{ 1 + \left[\frac{(II_{\dot{E}p})^{\frac{1}{2}}}{Y_0} \left(\frac{(II_{\dot{E}})^{\frac{1}{2}}}{10^{-4}} - 1 \right) \right]^{\frac{1}{5}} \right\}$
$\varkappa_0 = 425$ N/mm²
$Y_0 = 1.8259459 \cdot 10^{10}\ s^{-1}$
$(II_E)^{\frac{1}{2}} = 0.12$
600
500
400
10^{-4} 10^{-3} 10^{-2} 10^{-1} 10^{0} 10^{1} 10^{2} 10^{3} $(II_{\dot{E}})^{\frac{1}{2}}$
(s^{-1})

Fig.13

we obtain results for mild steel (plotted in Fig.12) and for low-carbon steel (plotted in Fig. 13).

A similar procedure is applied basing on the results obtained in dynamical tests performed under one-dimensional loading. For this case an optimum criterion is as follows

$$\mathcal{T} = \max_{\substack{t \in [0, d_p] \\ \dot{E} \in (\dot{E}_s, \dot{E}_{max}]}} \left\| T(t) - \hat{\mathcal{G}}(\dot{E}(t)) \Big|_{E = const} \right\| , \tag{8.4}$$

where

$$T(t) = \varkappa^* \left\{ 1 + \Phi^{-1} \left[\frac{\dot{E}}{\gamma_o} * \varphi \left(\frac{\dot{E}}{\dot{E}_s} - 1 \right) \right] \right\} \tag{8.5}$$

and

$$T(t) = \hat{\mathcal{G}}(\dot{E}(t)) \Big|_{E = const} \tag{8.6}$$

represents the experimental curve obtained for $E = const.$

The results obtained for mild steel basing on CAMPBELL and FERGUSON [8] data are plotted in Fig.14 and for plain carbon steel basing on experimental tests performed by different authors (cf. KANNINEN, MUKHERJEE, ROSENFIELD and HAHN [24]) are shown in Fig.15 .

The previously discussed procedure has been generalized to the elastic-work hardening viscoplastic material in Ref. [39] . It has been assumed that

$$\dot{E}_p = \frac{\gamma(E_p)}{\frac{\dot{E}_p}{\dot{E}_p^s} - 1} \left\langle \left(\frac{T}{\hat{Y}(E_p)} - 1 \right)^n \right\rangle \tag{8.7}$$

and

$$\gamma(E_p) = \gamma_o + a E_p^2 , \tag{8.8}$$

$$\hat{Y}(E_p) = Y_{so} + K E_p^b .$$

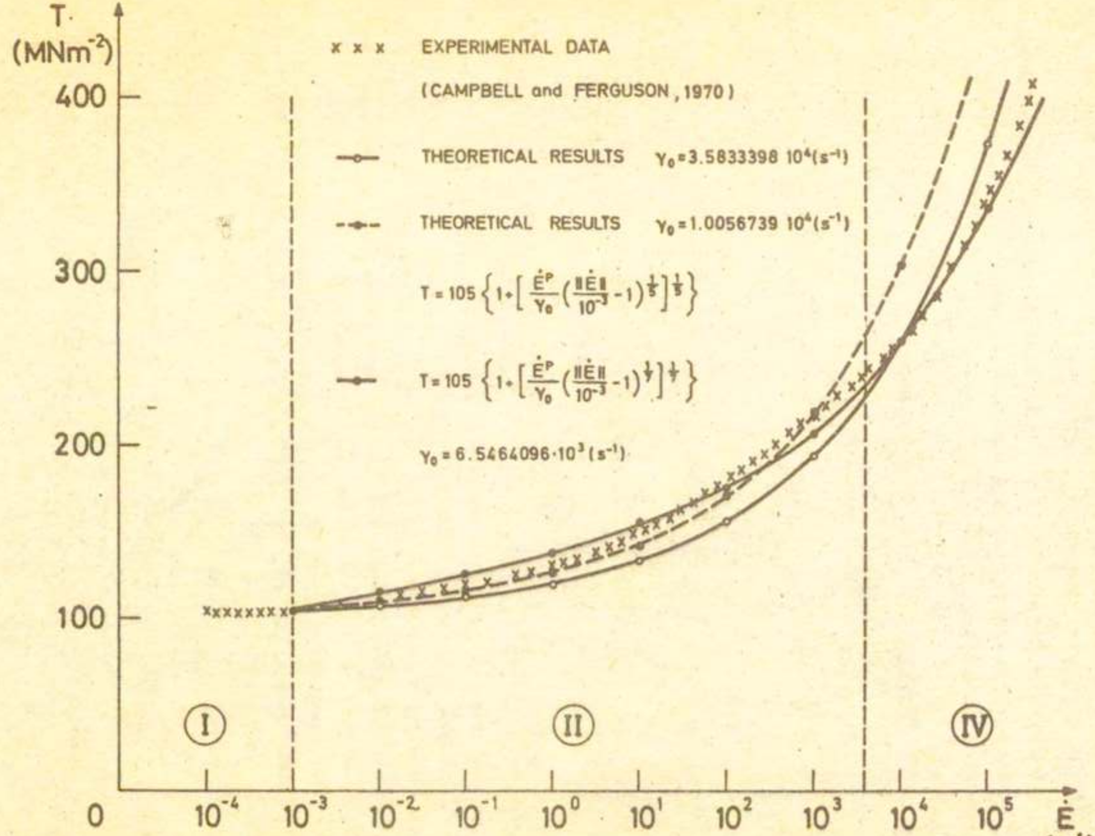
T (MNm^-2)
400
300
200
100
0
x x x EXPERIMENTAL DATA
(CAMPBELL and FERGUSON, 1970)
THEORETICAL RESULTS $\gamma_0 = 3.5833398 \; 10^4 (s^{-1})$
THEORETICAL RESULTS $\gamma_0 = 1.0056739 \; 10^4 (s^{-1})$
$T = 105 \left\{ 1 + \left[\frac{\dot{E}^P}{\gamma_0} \left(\frac{\|\dot{E}\|}{10^{-3}} - 1 \right)^{\frac{1}{5}} \right]^{\frac{1}{5}} \right\}$
$T = 105 \left\{ 1 + \left[\frac{\dot{E}^P}{\gamma_0} \left(\frac{\|\dot{E}\|}{10^{-3}} - 1 \right)^{\frac{1}{7}} \right]^{\frac{1}{7}} \right\}$
$\gamma_0 = 6.5464096 \cdot 10^3 (s^{-1})$
I
II
IV
10^{-4} 10^{-3} 10^{-2} 10^{-1} 10^{0} 10^{1} 10^{2} 10^{3} 10^{4} 10^{5}
$\dot{E}$ (s^{-1})

Fig.14

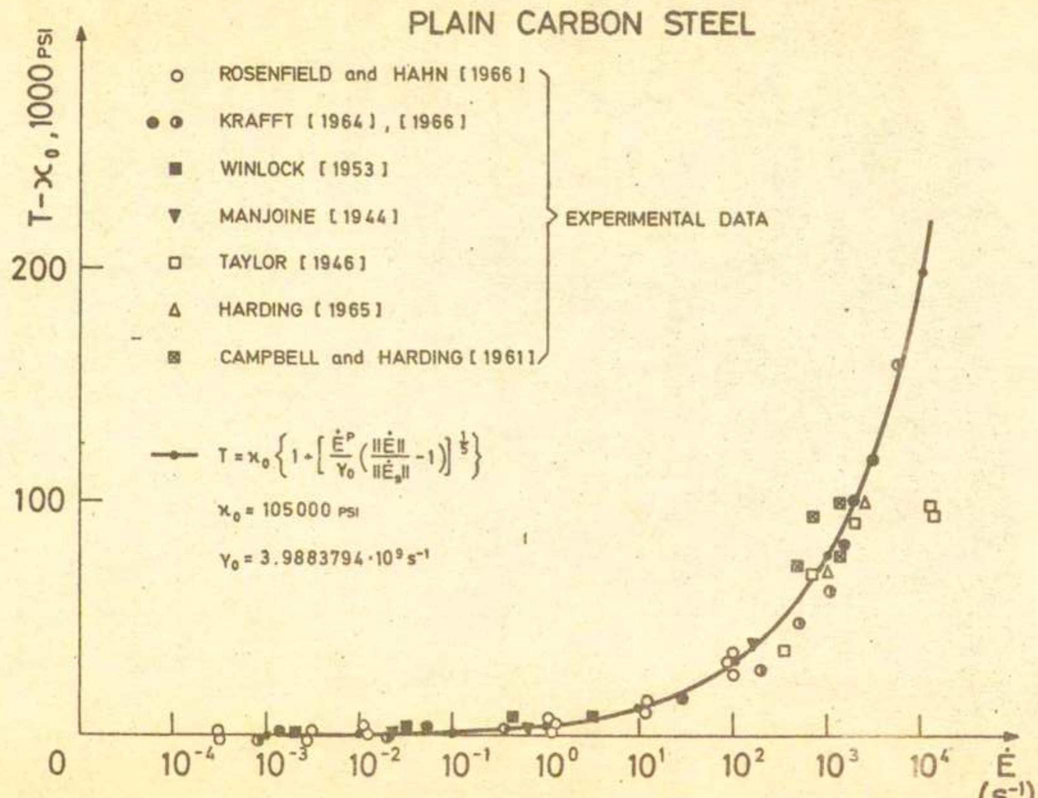
PLAIN CARBON STEEL
T−x₀, 1000 PSI
200
100
0
ROSENFIELD and HAHN [1966]
KRAFFT [1964], [1966]
WINLOCK [1953]
MANJOINE [1944]
TAYLOR [1946]
HARDING [1965]
CAMPBELL and HARDING [1961]
EXPERIMENTAL DATA
$T = x_0 \left\{ 1 + \left[\frac{\dot{E}^P}{Y_0} \left(\frac{\|\dot{E}\|}{\|\dot{E}_s\|} - 1 \right) \right]^{\frac{1}{5}} \right\}$
$x_0 = 105000$ PSI
$Y_0 = 3.9883794 \cdot 10^9 s^{-1}$
10^{-4} 10^{-3} 10^{-2} 10^{-1} 10^{0} 10^{1} 10^{2} 10^{3} 10^{4}
$\dot{E}$ (s^{-1})
Fig.15

The equation (8.7) gives the relation for the dynamic yield stress as follows

$$T = \hat{Y}(E_p)\left\{1+\left[\frac{1}{\gamma(E_p)}\left(\frac{\dot{E}_p^2}{\dot{E}_p^s}-1\right)\right]^{1/n}\right\} . \qquad (8.9)$$

To fit data obtained[12/] by ALBERTINI and MONTAGNANI [2] it has been found

$$n = 7, \quad \gamma_o = 1.5 \cdot 10^9 \left[s^{-1}\right], \quad a = 9.8 \cdot 10^{11} \left[s^{-1}\right],$$

$$Y_{so} = 25\left[\frac{kG}{mm^2}\right], \quad K = 50\left[\frac{kG}{mm^2}\right], \quad b = 0.38 .$$

The comparison of theoretical predictions with experimental data are given in Figs. 16 and 17.

8.2. Basing on metallurgical observations. There are very few available data concerning the quantitative void measurements during tensile test. FISHER [13] was conducted an investigation to determine the effects of various mechanical and material parameters on void formation at cementite particles in axisymmetric tensile specimens of spheroidized plain carbon steel. The volume fraction of voids $\xi = f_v$ and the number of voids per unit area of transverse cross section η_A , were measured as functions of deformation in the neck of each specimen, Figs. 18 and 19.

Similar data have been recently obtained by LE ROY, EMBURY, EDWARD and ASHBY [25] for spheroidized steels (cf. Figs. 7 and 8).

To determine the constant matrix $\underset{\sim}{\Xi}_o$, the constant l and the material function h in evolution equation for the imperfection parameter ξ we use FISHERS data.

The material function h and constants $\underset{\sim}{\Xi}_o$ and l are obtained by using the best curve-fitting method (as it is shown in Fig.18).

12/ Cf. also data presented by ALBERTINI, DEL GRANDE and MONTAGNANI [1] and ALBERTINI, MONTAGNANI, CENERINI and CURIONI [3].

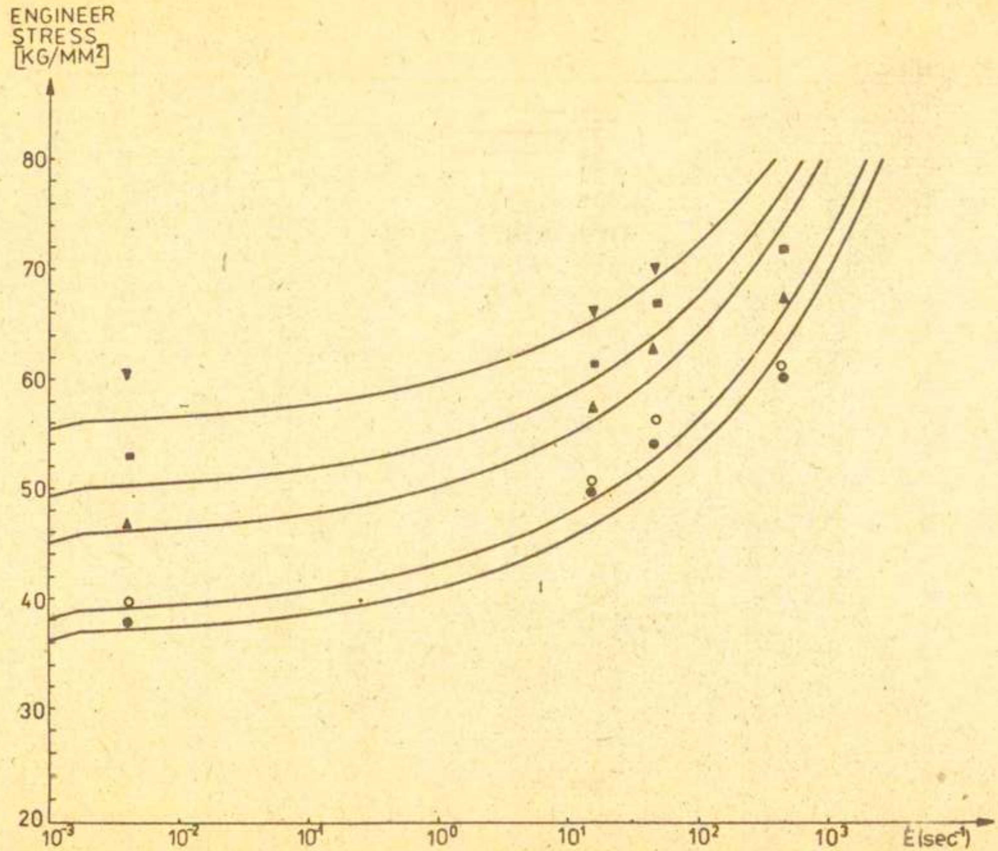
ENGINEER
STRESS
[KG/MM²]
80
70
60
50
40
30
20
10⁻³
10⁻²
10⁻¹
10⁰
10¹
10²
10³
ε̇ (sec⁻¹)

Fig.16

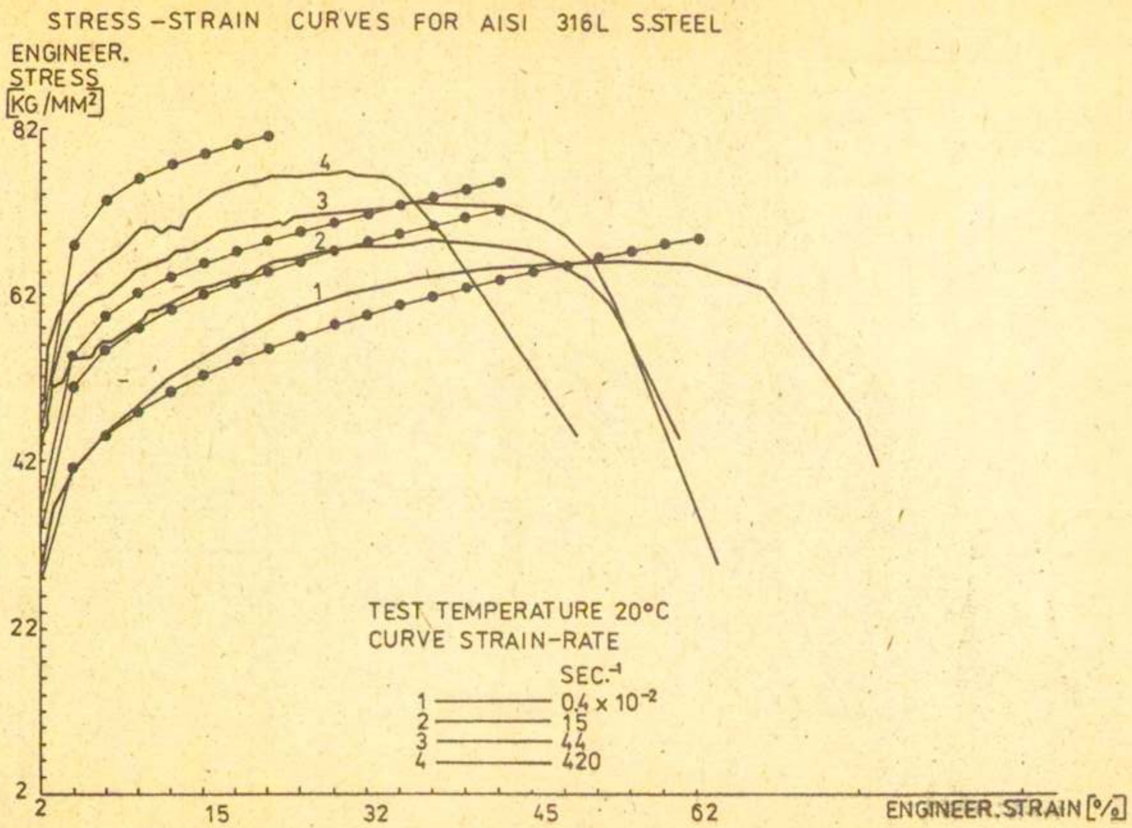
STRESS -STRAIN CURVES FOR AISI 316L S.STEEL
ENGINEER.
STRESS
[KG/MM²]
82
62
42
22
2
2
15
32
45
62
ENGINEER. STRAIN [%]
4
3
2
1
TEST TEMPERATURE 20°C
CURVE STRAIN-RATE
SEC.⁻¹
1 0.4 x 10⁻²
2 15
3 44
4 420

Fig.17

It is worthwile to compare our theoretical predictions with those presented by SAJE, PAN and NEEDLEMAN [45] based also on Fisher's data, cf. Fig. 20.

9. Necking phenomena

9.1. Formulation of the initial-boundary-value problem. Let us study the tensile deformation of a circular cylindrical bar of initial length $2L_0$ and initial radius R_0, cf. Fig. 21. The problem is described in the cylindrical coordinates r, θ, z. It has been assumed that the problem is axisymmetric and additionally that the deformations are symmetric about the mid plane $z = 0$. The ends of the specimen are assumed to remain shear free.

We use the Eulerian spatial description and the rate type constitutive modelling.

The problem is formulated for the two different yield functions assumed.

In the first case $f(\cdot)=(J_2')^{1/2}$ we have the constitutive evolution equations as follows

$$\frac{1}{2G}\left[\frac{\partial\sigma_{rr}}{\partial t} + v_r\frac{\partial\sigma_{rr}}{\partial r} + v_z\frac{\partial\sigma_{rr}}{\partial z} - \frac{\nu}{1+\nu}\,\mathrm{tr}(\overset{\nabla}{\underset{\sim}{\sigma}})\right]$$

$$= \frac{\partial v_r}{\partial r} - \frac{\gamma_0}{\varphi\left(\frac{I_2}{I_2^s}-1\right)}\left\langle \Phi\left[\frac{\sqrt{J_2'}}{\varkappa_0(1-\xi^{1/2})} - 1\right]\right\rangle \frac{S_{rr}}{\sqrt{J_2'}}\,,$$

$$\frac{1}{2G}\left[\frac{\partial\sigma_{\theta\theta}}{\partial t} + v_r\frac{\partial\sigma_{\theta\theta}}{\partial r} + v_z\frac{\partial\sigma_{\theta\theta}}{\partial z} - \frac{\nu}{1+\nu}\,\mathrm{tr}(\overset{\nabla}{\underset{\sim}{\sigma}})\right]$$

$$= \frac{v_r}{r} - \frac{\gamma_0}{\varphi}\left\langle \Phi[\;]\right\rangle \frac{S_{\theta\theta}}{\sqrt{J_2'}}\,,$$

$$\frac{1}{2G}\left[\frac{\partial\sigma_{zz}}{\partial t} + v_r\frac{\partial\sigma_{zz}}{\partial r} + v_z\frac{\partial\sigma_{zz}}{\partial z} - \frac{\nu}{1+\nu}\,\mathrm{tr}(\overset{\nabla}{\underset{\sim}{\sigma}})\right]$$

$$= \frac{\partial v_z}{\partial z} - \frac{\gamma_0}{\varphi}\left\langle \Phi[\;]\right\rangle \frac{S_{zz}}{\sqrt{J_2'}}$$

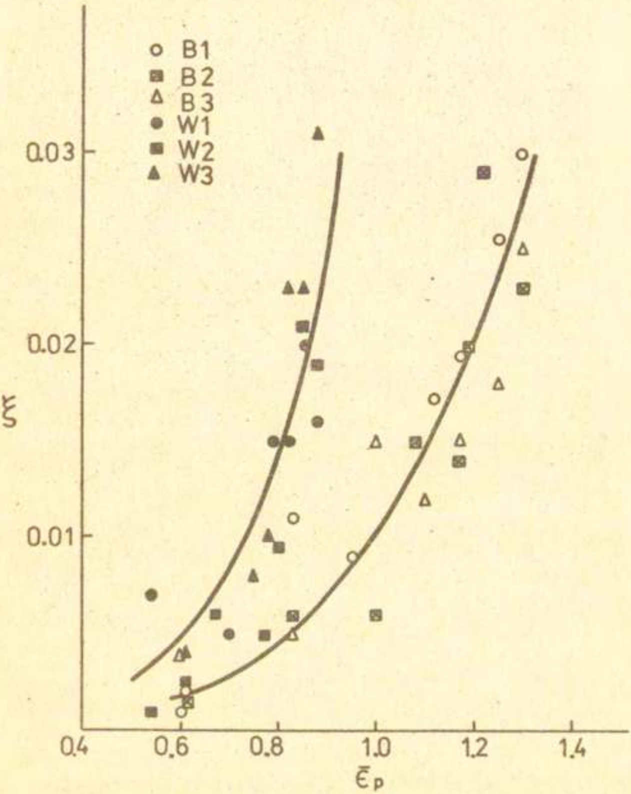

Fig. 18

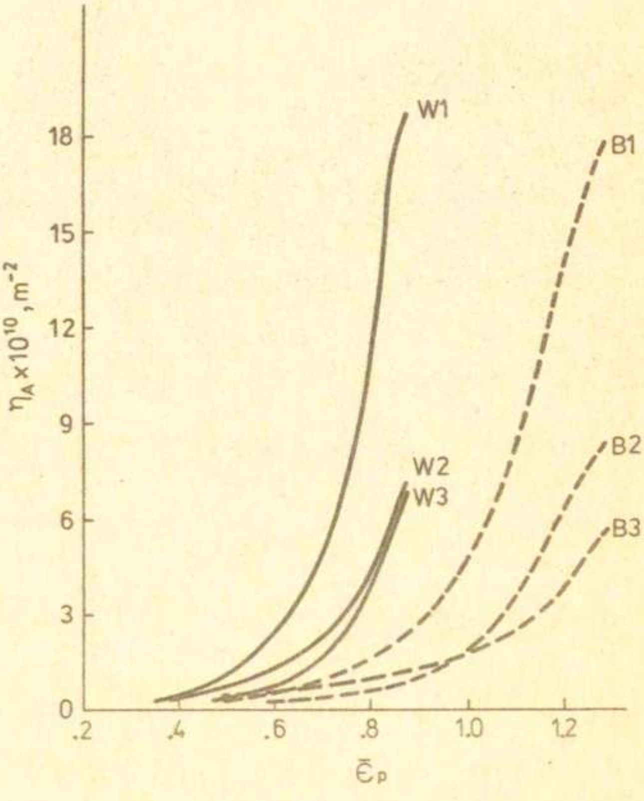
W1
B1
W2
W3
B2
B3
18
15
12
9
6
3
0
.2
.4
.6
.8
1.0
1.2
$\eta_A \times 10^{10}$, m^{-2}
$\bar{\epsilon}_p$

Fig.19

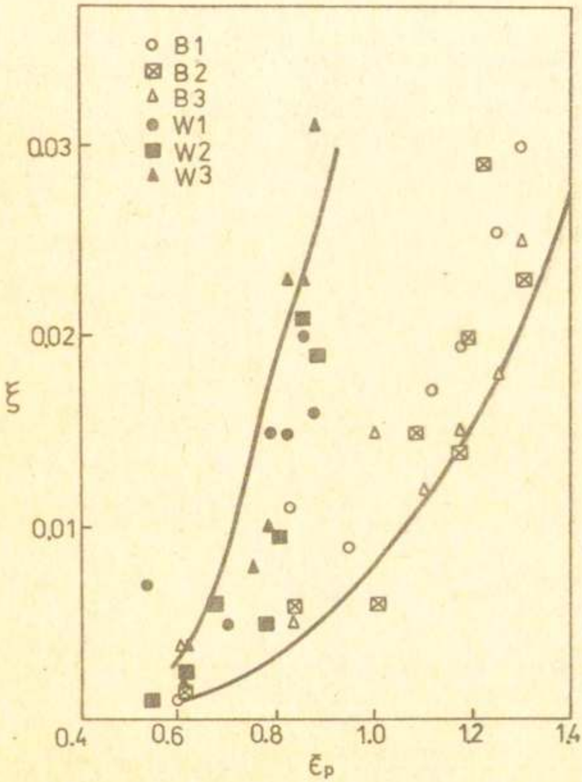

Fig.20

INITIAL-BOUNDARY VALUE PROBLEM
(ELASTIC-VISCOPLASTIC FLOW PROCESS)

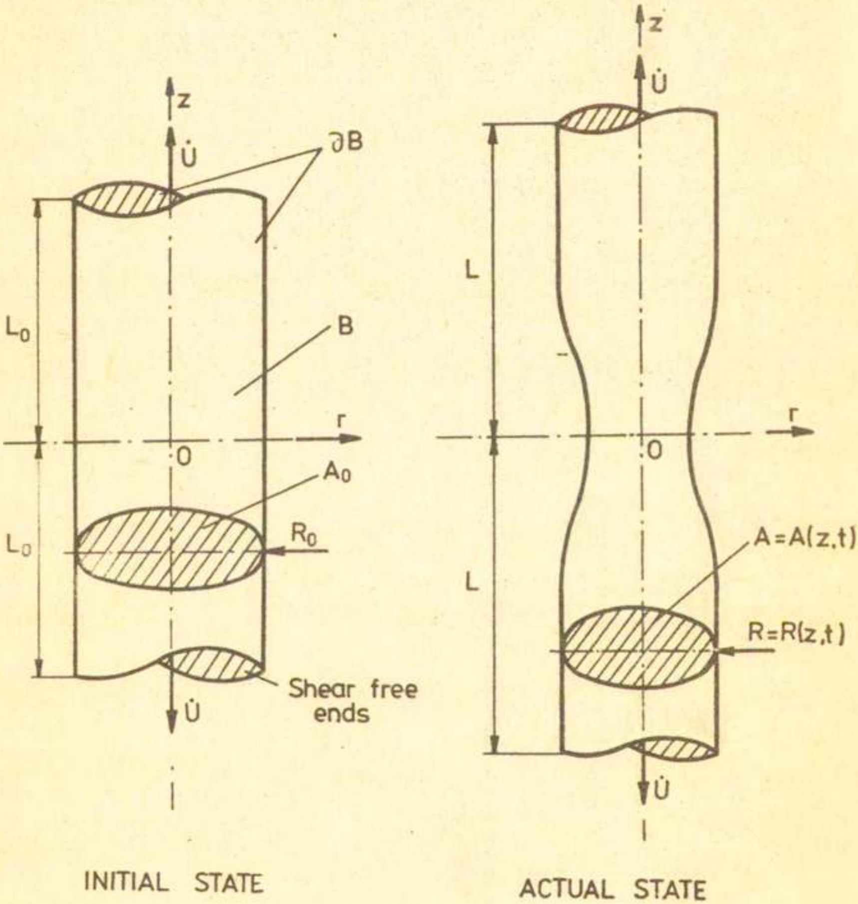

Fig. 21

$$\frac{1}{2G}\left(\frac{\partial\sigma_{rz}}{\partial t}+v_r\frac{\partial\sigma_{rz}}{\partial r}+v_z\frac{\partial\sigma_{rz}}{\partial z}\right)=\frac{\partial v_r}{\partial z}+\frac{\partial v_z}{\partial r}$$
$$-\frac{\gamma_0}{\varphi}\left\langle\Phi\left[\;\right]\right\rangle\frac{\sigma_{rz}}{\sqrt{J_2^1}}\,.$$

For the second case $f(\cdot)=J_2^1+n\xi J_1^2$ the constitutive evolution equations take the form

$$\frac{1}{2G}\left[\frac{\partial\sigma_{rr}}{\partial t}+v_r\frac{\partial\sigma_{rr}}{\partial r}+v_z\frac{\partial\sigma_{rr}}{\partial z}-\frac{\nu}{1+\nu}\operatorname{tr}(\overset{\nabla}{\underset{\sim}{\sigma}})\right]$$

$$=\frac{\partial v_r}{\partial r}-\frac{\gamma_0}{\varphi\left(\frac{I_2}{I_2^s}-1\right)}\left\langle\Phi\left[\frac{J_2^1+n\xi J_1^2}{\varkappa_0^2(1-\xi^{1/2})}-1\right]\right\rangle\frac{S_{rr}+2n\xi J_1}{\varkappa_0}\,,$$

$$\frac{1}{2G}\left[\frac{\partial\sigma_{\theta\theta}}{\partial t}+v_r\frac{\partial\sigma_{\theta\theta}}{\partial r}+v_z\frac{\partial\sigma_{\theta\theta}}{\partial z}-\frac{\nu}{1+\nu}\operatorname{tr}(\overset{\nabla}{\underset{\sim}{\sigma}})\right] \qquad (9.2)$$

$$=\frac{v_r}{r}-\frac{\gamma_0}{\varphi}\left\langle\Phi\left[\;\right]\right\rangle\frac{S_{\theta\theta}+2n\xi J_1}{\varkappa_0}\,,$$

$$\frac{1}{2G}\left[\frac{\partial\sigma_{zz}}{\partial t}+v_r\frac{\partial\sigma_{zz}}{\partial r}+v_z\frac{\partial\sigma_{zz}}{\partial z}-\frac{\nu}{1+\nu}\operatorname{tr}(\overset{\nabla}{\underset{\sim}{\sigma}})\right]$$

$$=\frac{\partial v_z}{\partial z}-\frac{\gamma_0}{\varphi}\left\langle\Phi\left[\;\right]\right\rangle\frac{S_{zz}+2n\xi J_1}{\varkappa_0}\,,$$

$$\frac{1}{2G}\left(\frac{\partial\sigma_{rz}}{\partial t}+v_r\frac{\partial\sigma_{rz}}{\partial r}+v_z\frac{\partial\sigma_{rz}}{\partial z}\right)=\frac{\partial v_r}{\partial z}+\frac{\partial v_z}{\partial r}$$

$$-\frac{\gamma_0}{\varphi}\left\langle\Phi\left[\;\right]\right\rangle\frac{\sigma_{rz}}{\varkappa_0}\,.$$

The evolution equation for the imperfection parameter is independent of the assumed yield condition and has the form

$$\frac{\partial \xi}{\partial t} + \frac{\partial \xi}{\partial r} v_r + \frac{\partial \xi}{\partial z} v_z = D_0 \Big[\frac{1}{r} \frac{\partial}{\partial r} \Big(r \frac{\partial \xi}{\partial r} \Big) + \frac{\partial^2 \xi}{\partial z^2} \tag{9.3}$$

$$+ (1-\xi) \operatorname{tr} (\underset{\sim}{\Xi}_0 \underset{\sim}{D}^p) + \frac{h}{1-\xi} \operatorname{tr} (\underset{\sim}{\sigma} \underset{\sim}{D}^p) + l\, j \ ,$$

The equations of motion are as follows

$$\rho \frac{\partial v_r}{\partial t} + \Big(\rho v_r \frac{\partial v_r}{\partial r} - \frac{\partial \sigma_{rr}}{\partial r} \Big) + \Big(\rho v_z \frac{\partial v_r}{\partial z} - \frac{\partial \sigma_{rz}}{\partial z} \Big)$$

$$- \frac{1}{r} (\sigma_{rr} - \sigma_{\theta\theta}) = 0 \tag{9.4}$$

$$\rho \frac{\partial v_z}{\partial t} + \Big(\rho v_r \frac{\partial v_z}{\partial r} - \frac{\partial \sigma_{rz}}{\partial r} \Big) + \Big(\rho v_z \frac{\partial v_z}{\partial z} - \frac{\partial \sigma_{zz}}{\partial z} \Big)$$

$$- \frac{1}{r} \sigma_{rz} = 0 \ .$$

The kinematical expressions have the form

$$v_r = \frac{\partial u_r}{\partial t} + v_r \frac{\partial u_r}{\partial r} + v_z \frac{\partial u_r}{\partial z} \ , \tag{9.5}$$

$$v_z = \frac{\partial u_z}{\partial t} + v_r \frac{\partial u_r}{\partial r} + v_z \frac{\partial u_z}{\partial z} \ .$$

The initial values for the problem considered are determined

$$t = 0 \ , \ r \in [0, R_0] \ , \ z \in [0, L_0] \ .$$

$$\underset{\sim}{u}(r,z,0) = 0 \ ,$$

$$\underset{\sim}{\sigma}(r,z,0) = 0 \ , \tag{9.6}$$

$$\xi(r,z,0) = \xi^0(r,z) \ .$$

The boundary conditions are postulated in the form:

(i) the lateral surface of the specimen is required to remain stress free during the straining process

$$\dot{t}^r = \left(\frac{\partial \hat{n}}{\partial t} + v_z \frac{\partial \hat{n}}{\partial z}\right)\left(\sigma_{rr} + \sigma_{rz}\frac{\partial R}{\partial z}\right) + \hat{n}(z,t)\left\{\frac{\partial \sigma_{rr}}{\partial t} + v_r \frac{\partial \sigma_{rr}}{\partial r} + v_z \frac{\partial \sigma_{rr}}{\partial z} + \frac{\partial^2 R}{\partial z \partial t}\sigma_{rz} + \frac{\partial R}{\partial z}\left(\frac{\partial \sigma_{rz}}{\partial t} + v_r \frac{\partial \sigma_{rz}}{\partial r} + v_z \frac{\partial \sigma_{rz}}{\partial z}\right)\right\} = 0$$

$$\dot{t}^z = \left(\frac{\partial \hat{n}}{\partial t} + v_z \frac{\partial \hat{n}}{\partial z}\right)\left(\sigma_{rz} + \sigma_{rz}\frac{\partial R}{\partial z}\right) + n(z\,t)\left\{\frac{\partial \sigma_{rz}}{\partial t} + v_r \frac{\partial \sigma_{rz}}{\partial r} + v_z \frac{\partial \sigma_{rz}}{\partial z} + \frac{\partial^2 R}{\partial z \partial t}\sigma_{zz} + \frac{\partial R}{\partial z}\left(\frac{\partial \sigma_{zz}}{\partial t} + v_r \frac{\partial \sigma_{zz}}{\partial r} + v_z \frac{\partial \sigma_{zz}}{\partial z}\right)\right\} = 0, \qquad (9.7)$$

$$\dot{t}^\theta = 0,$$

for $t \in [0, d_p]$, $r = R(z,t)$, $z \in [0, L(t)]$, where

$$n_r = \hat{n}(z,t), \quad n_z = \frac{\partial R}{\partial z}\hat{n}(z,t) \qquad (9.8)$$

and

$$\hat{n}(z,t) = \left[\left(\frac{\partial R}{\partial z}\right)^2 - 1\right]^{-\frac{1}{2}}; \qquad (9.9)$$

(ii) the specimen has shear-free ends

$$\dot{t}_r = \left[\frac{\partial \sigma_{rz}}{\partial t} + v_r \frac{\partial \sigma_{rz}}{\partial r} + v_z \frac{\partial \sigma_{rz}}{\partial z}\right]_{z=L(t)} = 0,$$

$$\dot{t}_\theta = 0, \qquad (9.10)$$

for $t \in [0, d_p]$, $r \in [0, R(z,t)]\Big|_{z=L(t)}$;

(iii) to the ends of the specimen is prescribed constant velocity $\dot{U}$ in direction of z axis, i.e.

$$\vartheta_r(r, L(t), t) = \dot{U},$$

$$\text{for} \quad t \in [0, d_p], \quad r \in [0, R(z,t)] \Big|_{z = L(t)} ; \qquad (9.11)$$

(iv) the assumed symmetry about $z = 0$ requires

$$\dot{t}_r(r,0,t) = 0, \quad \dot{t}_\theta(r,0,t) = 0 \quad \vartheta_z(r,0,t) = 0$$

$$\text{for} \quad t \in [0,d_p], \quad r \in [0, R(0,t)]; \qquad (9.12)$$

(v) the imperfection parameter has to satisfy the boundary condition as follows

$$\underline{a}\, \partial_B \xi(r,z,t) + b\, \xi(r,z,t) = 0$$

for

$$t \in [0,d_p], \quad r = R(z,t), \quad z \in [0,L(t)], \qquad (9.13)$$

and for $t \in [0,d_p]$, $r \in [0,R(z,t)]$, $z = L(t)$,

i.e. for the lateral surface as well as for the end surfaces.

The necking problem is described by the evolution equations for the components of the Cauchy stress tensor (9.1) or (9.2) the evolution equation for the imperfection parameter (9.3), the equations of motion (9.4), the kinematic equations (9.5) the initial values (9.6) and the boundary conditions (9.7) - (9.13).

The solution of the initial-boundary-value problem is represented in the cylindrical coordinates system by

$$\underset{\sim}{\varphi} = \{u_r, u_z, \vartheta_r\, \vartheta_z, \sigma_{rr}, \sigma_{\theta\theta}, \sigma_{zz}, \sigma_{rz}, \xi\}(r,z,t) \, . \qquad (9.14)$$

The problem formulated is very complex. So, it is worth while to consider some particular cases which can be treated as reasonable simplifications of the general problem.

9.2. Influence of the strain rate effect on the onset of localization. Let us assume that there is no internal imperfections in the material of the specimen and let consider a sequence of the initial-boundary-value problems by postulating

$$\mathcal{V}_z\,(r,\,L\,(t),\,t) = \dot{U}_1\,,\,\dot{U}_2,\,\ldots\ldots,\,\dot{U}_n, \tag{9.15}$$

instead of the condition (9.11).

The spectrum of velocities $\dot{U}_1$, $\dot{U}_2$, $\dot{U}_3$ ......, $\dot{U}_n$ has to be assumed such that it causes changes of the mean strain rate in the specimen in a sufficiently large range.

To simplify the numerical procedure as far as possible let us neglect the inertial terms in the equations of motion (9.4). So, we shall treat problem as quasi-static (cf. Ref. [34]).

Since the problem has been simplified to quasi-static, we have to restrict our considerations to such values of the velocities $\dot{U}_i$ ($i = 1,2, \ldots\ldots, n$) to be sure that our quasi-static approximation is valid.

The advantage of the problem posed in Sec. 9.1 is the unified formulation for the elastic-viscoplastic range as well as for the elastic-plastic response of a material. So, we can obtain the Needleman results as a limit case of our processes under the assumption that the velocity $\dot{U}_1 = \dot{U}_{static} = \dot{U}$ (assumed by Needleman [28]).

The numerical results obtained are plotted in Figs. 22 and 23. These theoretical results can be compared with experimental data obtained for 316 L stainless steel by ALBERTINI and MONTAGNANI [2] (cf. also Fig.16) and which are presented in Figs. 24 and 25.

It can be said that the theoretical predictions are consistent with experimental observations that the load at the instability point is increasing function of the strain rate while the strain at the same point is decreasing function of the strain rate.

9.3. Influence of imperfections on the elastic-plastic-solution. We shall now consider the elastic-plastic response of a material with internal imperfections. In the evolution equation (9.3) for the imperfection parameter we neglect the diffusional term (as it has been postulated for the elastic-plastic range, cf. Sec. 7).

The numerical finite-difference procedure may be developed in such a way that it can be applicable for all the yield functions postulated by Eqs. (6.19). However, since we are interested

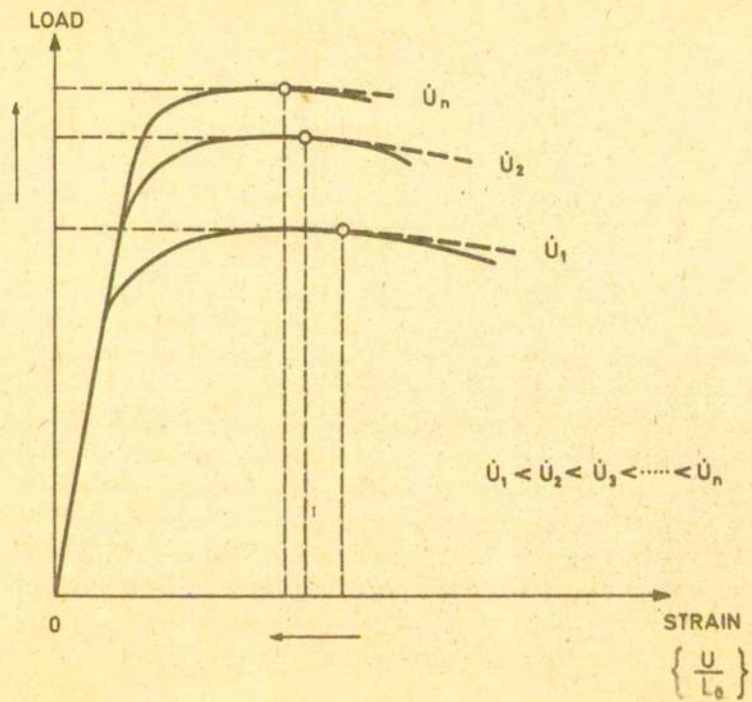
LOAD
$\dot{U}_n$
$\dot{U}_2$
$\dot{U}_1$
$\dot{U}_1 < \dot{U}_2 < \dot{U}_3 < \cdots < \dot{U}_n$
0
STRAIN
$\left\{ \frac{U}{L_0} \right\}$

Fig.22

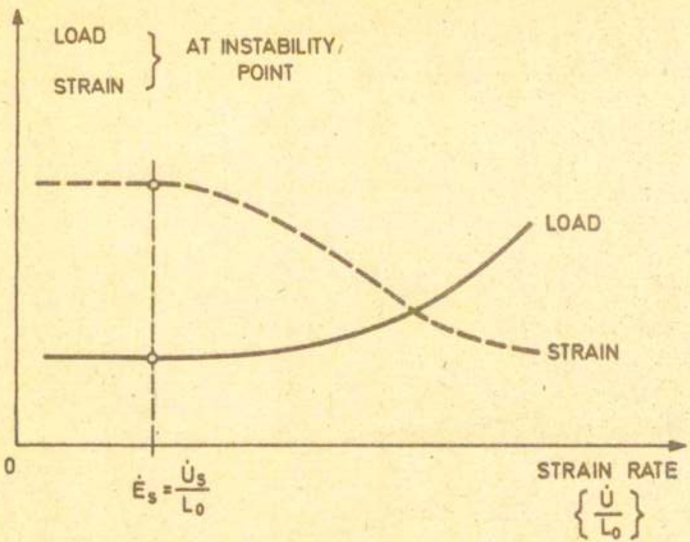
LOAD
STRAIN
AT INSTABILITY POINT
LOAD
STRAIN
0
$\dot{E}_s = \frac{\dot{U}_s}{L_0}$
STRAIN RATE
$\left\{ \frac{\dot{U}}{L_0} \right\}$

Fig. 23

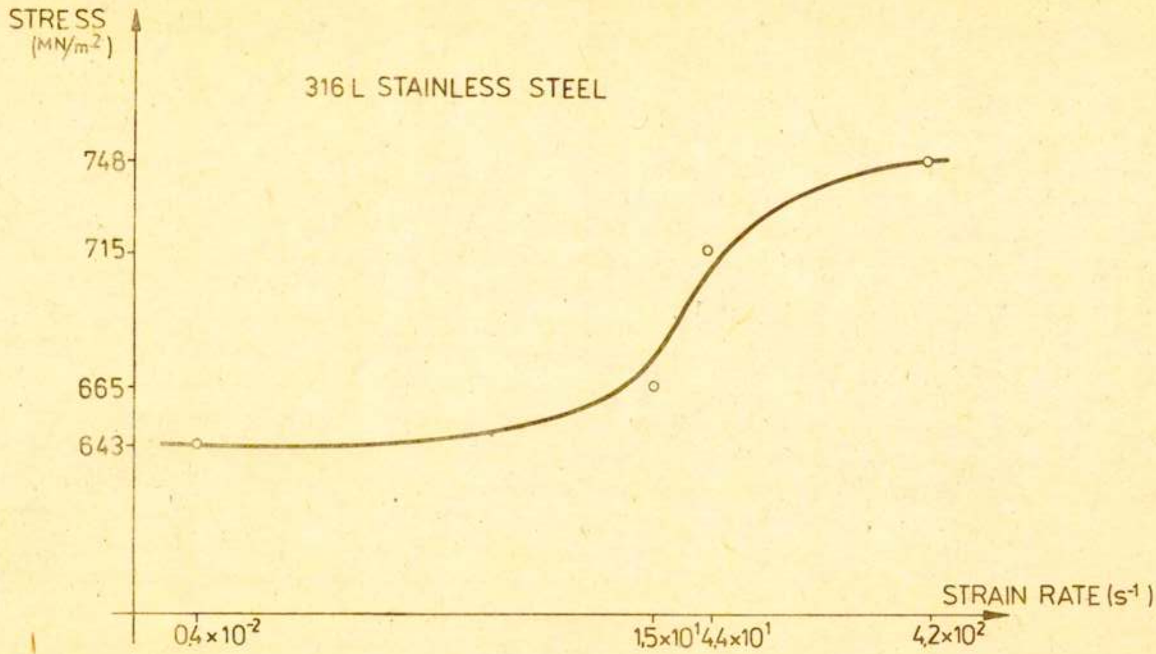
STRESS
(MN/m2)
316 L STAINLESS STEEL
748
715
665
643
0,4×10-2
1,5×10¹
4,4×10¹
4,2×10²
STRAIN RATE (s-1)

Fig.24

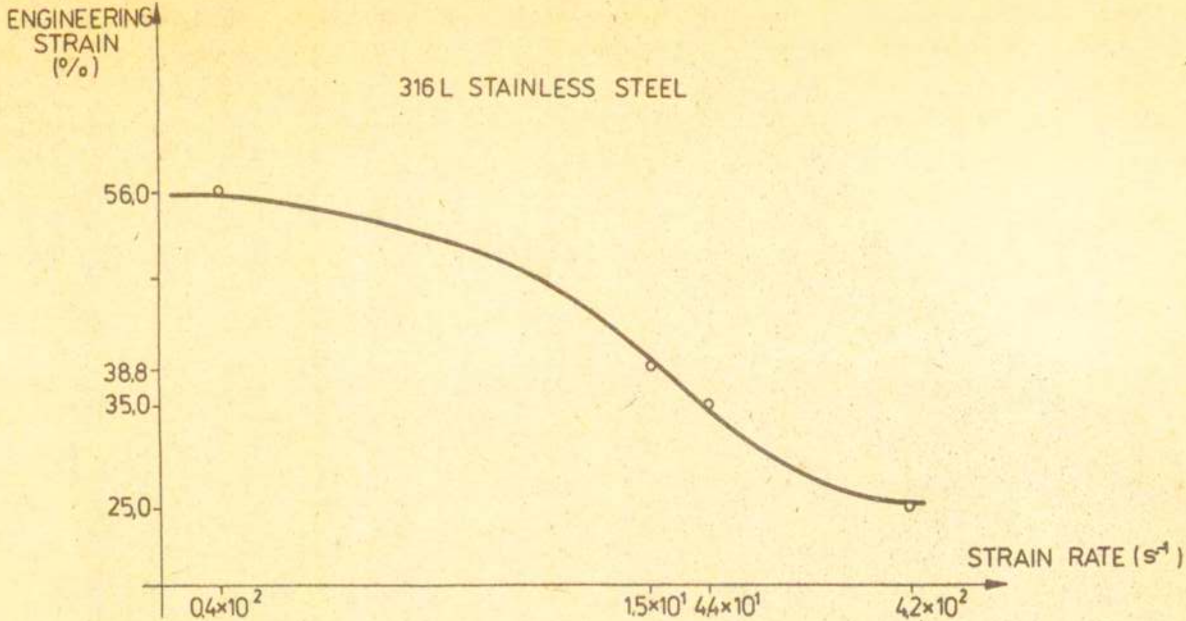
ENGINEERING
STRAIN
(%)
316 L STAINLESS STEEL
56,0
38,8
35,0
25,0
STRAIN RATE (s⁻¹)
0,4×10²
1,5×10¹
4,4×10¹
4,2×10²

Fig.25

in the comparison of our results for voided solids material with imperfections with those obtained by NEEDELMAN [28] we intend to focus our attention on the J_2' flow theory, i.e. we assume the yield condition in the form

$$(J_2')^{1/2} = \varkappa \quad , \qquad (9.16)$$

where $\varkappa$ is the work - hardening parameter.

It is postulated the engineering criterion of the onset of necking in the form of a maximum load condition(cf. Sec.3).

We postulate also that the process of deformation of the specimen is the same as that considered by NEEDLEMAN [28] until the maximum load point is reached. Starting from this point we superpose internal imperfections by postulating the following distribution of the initial imperfections

$$\overset{o}{\xi}(r,z) = 0.02\left(1 - \frac{r}{R}\right)\left(1 - \frac{z}{L}\right). \qquad (9.17)$$

This linear approximation is based on the experimental observations presented by FISHER [13] . He has performed quantitative void measurements during the tensile test. The areal density of voids η_A , measured as number of voids per unit area of transverse section, and the volume fraction of voids f_v are plotted as functions of z (with $r = 0$) and of r (with $z = 0$) for each specimen in Figs. 26, 27 and 28.

The material function

$$\varkappa = \hat{\varkappa}(\xi) \qquad (9.18)$$

is assumed in two particular forms, giving the parabolic and linear appro imations, cf. Fig. 29.

The results for voided elastic-plastic solid are compared with those obtained by NEEDLEMAN [28] in Fig. 30. Similar comparison has been presented for the first material function, i.e. for $\varkappa = \varkappa_0(1 - \xi^{1/2})$ in Fig.31. The latter results show the development of neck as a function of engineering strain.

FISHER [13] has presented the relationship between the equivalent plastic strain $\bar{\varepsilon}_p$ and z/L based on the numerical results of NEEDLEMAN [28] and the measurements of the neck contours of the B and W type specimens. Comparison of these results with our theoretical predictions for W type specimen has been shown in Fig. 32. This comparison shows that our theoretical results are consistent with Fisher's experimental observations.

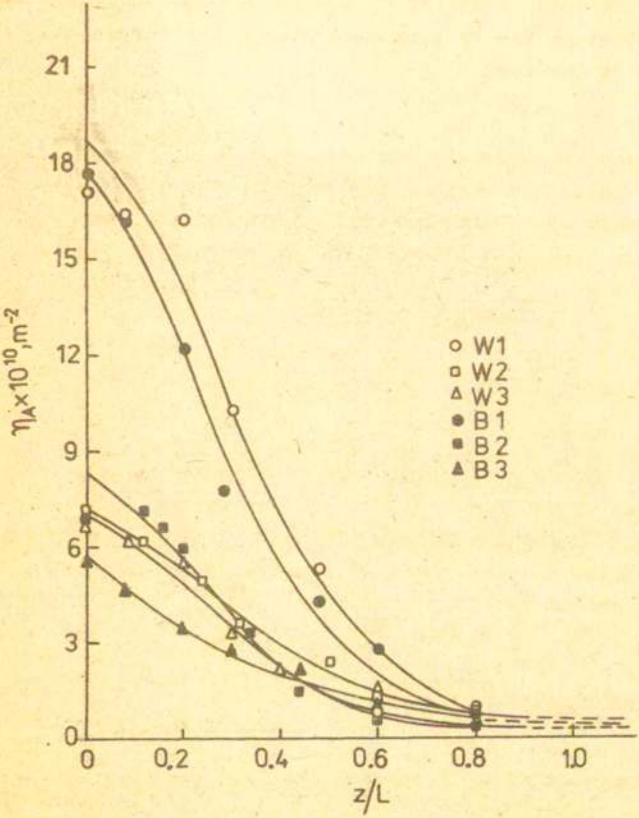

21
18
15
12
9
6
3
0
$\eta_A \times 10^{10}, m^{-2}$
W1
W2
W3
B1
B2
B3
0
0.2
0.4
0.6
0.8
1.0
z/L

Fig.26

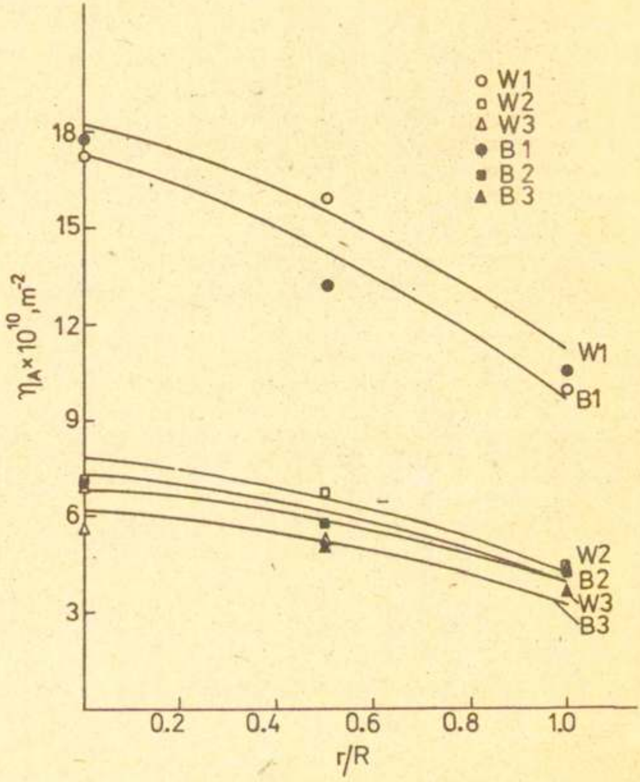
W1
W2
W3
B1
B2
B3
18
15
12
9
6
3
$\eta_A \times 10^{10}$, m^{-2}
W1
B1
W2
B2
W3
B3
0.2
0.4
0.6
0.8
1.0
r/R

Fig.27

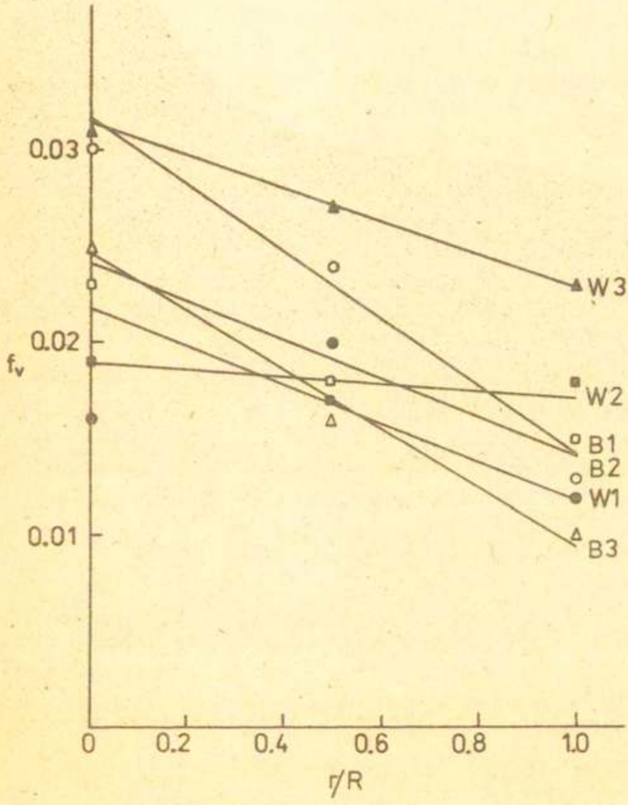

Fig.28

9.4. Influence of diffusion effects. To investigate the diffusional effects on the onset of necking as well as on the postcritical behaviour of the specimen we have to solve the initial-boundary-value problem (with inertial terms neglected) formulated in Sec. 9.1 for an elastic-viscoplastic material with internal imperfections. The evolution equation for the imperfection parameter ξ may be assumed in general form (9.3) with diffusional term included.

This problem enables us to show importance of the diffusional effects on the solution and to discuss cooperative effects by taking into consideration the strain rate sensitivity of the material as well as the internal imperfections.

Preliminary numerical results obtained for the problem posed prowed importance of the diffusional effects. However, the solution of the problem is very difficult to achieve numerically and it needs particular fine numerical procedure. So, it has to be postponed to further investigations.

10. Conclusions and comments

The main objective of the paper was to describe some cooperative phenomena generated by nucleation, growth and diffusion of voids during a deformation process for postcritical behaviour of dissipative solids.

Studies (cf. FISHER [13]) dealing with the deformation of solids containing dispersions of hard second phases or inclusions have shown that the nucleation of microcracks or voids is associated with these particles when the material of a body is subjected to various types of deformation. These voids appear either as cracks in the particles or as failures of the particle-matrix interfacial bonding. The actual void morphology depends upon the interrelation of various microstructural parameters as well as the local deformation state. In very high purity materials, the absence of particles acting as void sites requires that other mechanisms of void nucleation be operative. It has been observed that in high purity silver and stainless steel voids are nucleated in the areas characterized by high dislocation densities. During high temperature creep deformation void formation may be associated with diffusion controled processes in which grain boundaries act

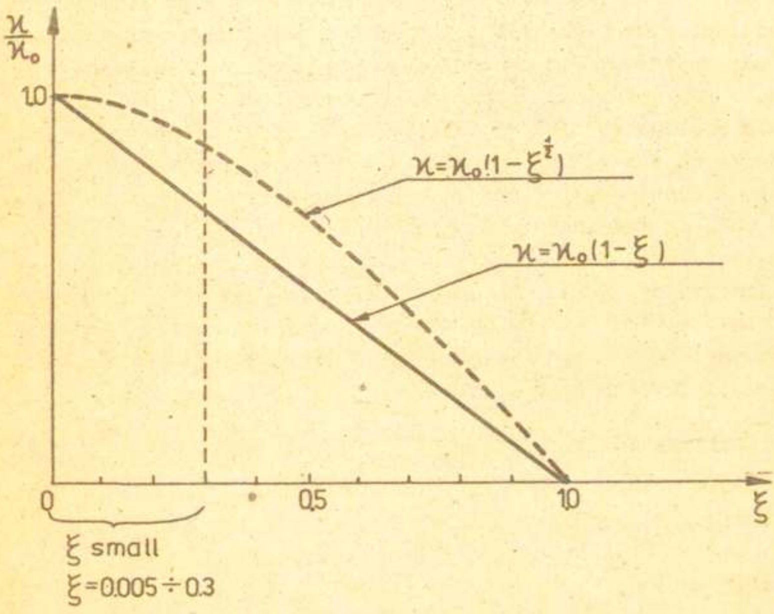

$\frac{\varkappa}{\varkappa_o}$
1.0
$\varkappa=\varkappa_o(1-\xi^{\frac{1}{2}})$
$\varkappa=\varkappa_o(1-\xi)$
0
0.5
1.0
ξ
ξ small
$\xi=0.005\div0.3$

Fig.29

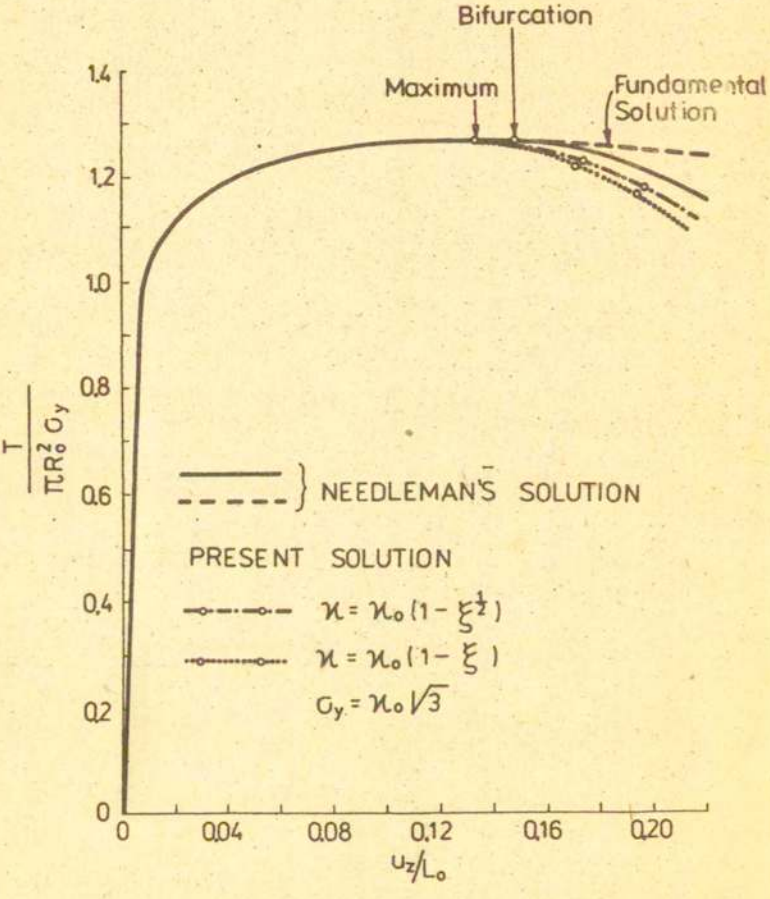
Bifurcation
Maximum
Fundamental Solution
1.4
1.2
1.0
0.8
0.6
0.4
0.2
0
$\frac{T}{\pi R_o^2 \sigma_y}$
NEEDLEMAN'S SOLUTION
PRESENT SOLUTION
$\varkappa = \varkappa_o (1 - \xi^{\frac{1}{2}})$
$\varkappa = \varkappa_o (1 - \xi)$
$\sigma_y = \varkappa_o \sqrt{3}$
0
0.04
0.08
0.12
0.16
0.20
u_z / L_o

Fig.30

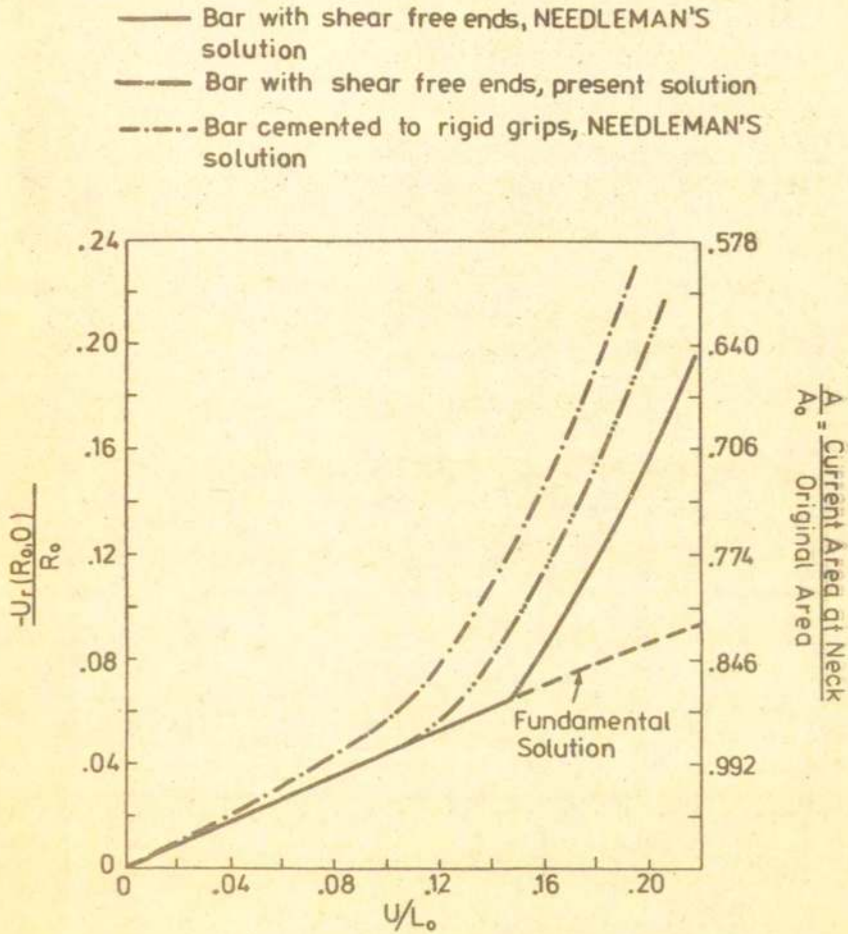

Bar with shear free ends, NEEDLEMAN'S solution
Bar with shear free ends, present solution
Bar cemented to rigid grips, NEEDLEMAN'S solution
.24
.20
.16
.12
.08
.04
0
.578
.640
.706
.774
.846
.992
0
.04
.08
.12
.16
.20
U/L₀
-U_r(R₀,0) / R₀
A/A₀ = Current Area at Neck / Original Area
Fundamental Solution

Fig.31

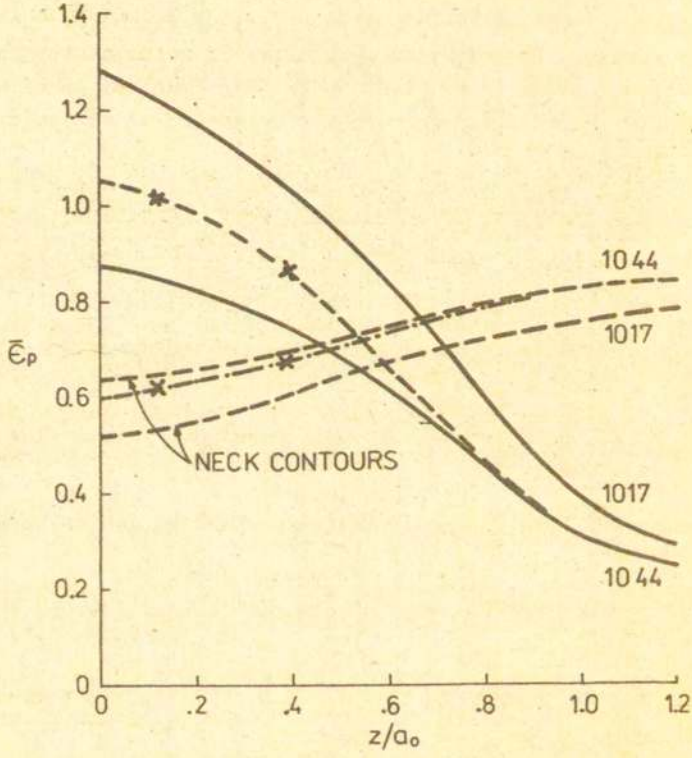

1.4
1.2
1.0
0.8
0.6
0.4
0.2
0
$\bar{\epsilon}_p$
1044
1017
NECK CONTOURS
1017
1044
0
.2
.4
.6
.8
1.0
1.2
z/a₀

Fig.32

as sinks and sources for vacancies with directional diffusion occuring as a result of the local stresses.

The theory proposed can describe such cooperative phenomena as influence of strain rate effects and imperfection and transport effects on main inelastic deformation process. However, this theory can not describe the final mechanism of fracture. The mechanism of fracture is initiated by linking of voids and by forming a long and narrow cavity within a body. This final stage of deformation process is of great practical importance and needs further study.

References

1. C. ALBERTINI, A. DEL GRANDE and M. MONTAGNANI, Effects of irradiation on the mechanical properties of austentic stainless steels under dynamic loading, ASTM, STP 683, Philadelphia 1979.

2. C. ALBERTINI and M. MONTAGNANI, Dynamic uniaxial and biaxial stress-strain relationship for austentic stainless steels, Nucl. Engn. Design, 57 , 107-123, 1980.

3. C. ALBERTINI, M. MONTAGNANI, R. CENERINI and S. CURIONI, Radiation, welding, temperature and strain rate influence on material properties in fast breeder reactors, Arch. Mechanics, 32 549-577, 1980.

4. R.J. ASARO, Micromechanics of crystals and polycrystals, Brown University Report, April 1982.

5. M.F. ASHBY, Micromechanisms of fracture in static and cylic failure, in Fracture Mechanics, Current Status, Future Prospects, Proc. Conference, Cambridge 1979, ed. R.A. Smith, Pergamon Press 1979, 1-27.

6. M.F. ASHBY, C. GANDI and D.M.R. TAPLIN, Fracture-mechanism maps and their construction for f.c.c. metals and alloys, Acta Metall., 27 , 699-729, 1979.

7. M.F. ASHBY and R.A. VERRALL, Diffusion-accommodated flow and superplasticity, Acta Metall., 21 , 149-163, 1973.

8. J.D. CAMPBELL and W.G. FERGUSON, The temperature and strain rate dependence of the shear strength of mild steel, Phil. Mag., 21, 63-82, 1970.

9. A.K. CHAKRABARTI and J.W. SPRETNAK, Instability of plastic flow in the direction of pure shear, Metall. Trans., 6A, 733-747, 1975.

10. R.L. COBLE, A model for boundary diffusion controlled creep in polycrystalline materials, J.Physics., 34, 1679-1682, 1967.

11. R.J. FIELDS, T. WEERASOORIYA and M.F. ASHBY, Fracture-mechanisms in pure iron, two austenitic steels and one ferritic steel, Metall. Trans. (in print).

12. C.P. FLYNN, Point defects and diffusion, Oxford 1972,

13. J.R. FISHER, Void nucleation in spheroidized steels during tensile deformation, Ph.D.Thesis, Brown University, 1980.

14. K. FRISCHMUTH and P. PERZYNA, Thermodynamics of modified material structure with internal state variables, Arch. Mechanics, 35, 1983, in print.

15. C. GANDHI and M.F. ASHBY, Fracture-mechanism maps for materials which cleave: f.c.c., b.c.c. and h.c.p. metals and ceramics; Acta Metall., 27, 1565-1602, 1979.

16. J. GURLAND, Observations on the fracture of cementite particles in a spheroidized 1.05% C steel deformed at room temperature, Acta Metall., 20, 735-741, 1972.

17. A.L. GURSON, Continuum theory of ductile rupture by void nucleation and growth, J.Eng. Materials and Tech., 99 2-15, 1977.

18. C. HERRING, Diffusonal viscosity of a polycrystalline solid, J. Appl. Phys., 21, 437-445, 1950.

19. R. HILL, Bifurcation and uniqueness in nonlinear mechanics of continua, in "Problems of Continuum Mechanics", N.I. Muskhelishvili Volume, 155-164, Soc. Ind. Appl. Math. Philadephia 1961.

20. R. HILL, Uniqueness in general boundary-value problems for elastic and inelastic solids, J. Mech.Phys. Solids, 9, 114-130, 1961; Uniqueness and extremum principles in self-adjoint boundary-value problems in continuum mechanics, J. Mech. Phys. Solids, 10, 185-194, 1962.

21. R. HILL, Aspects of invariance in solid mechanics, Advances in Applied Mechanics, 18, 1-73, 1978.

22. R. HILL and J.W. HUTCHINSON, Bifuraction phenomena in the plane strain tension test, J.Mech. Phys. Solids, 23, 239-264, 1975.

23. D. HULL and D.E. RIMMER, The growth of grain-boundary voids under stress, Phil. Mag., 4, 673-687, 1959.

24. M.F. KANNINEN, A.K. MUKHERJEE, A.R. ROSENFIELD and G.T. HAHN The speed of ductile-crack propagation and the dynamics of flow in metals, Proc. Symp. on Mechanical Behaviour of Materials under Dynamic Loads, San Antonio, September 1967, Springer, 96-133, 1968.

25. G. LE ROY, J.D. EMBURY, G. EDWARD and M.F. ASHBY, A model of ductile fracture based on the nucleation and growth of voids, Acta Metall., 29, 1509-1522, 1981.

26. U.S. LINDHOLM, Dynamic deformation of metals, in "Behaviour of Materials under Dynamic Loads, 42-61, ASME, New York 1965.

27. J.P. MILES, On necking phenomena and bifurcation solutions, Arch. Mechanics, 32, 909-931, 1980.

28. A. NEEDLEMAN, A numerical study of necking in circular cylindrical bars, J.Mech. Phys. Solids, 20,

29. A. NEEDLEMAN and J.R. RICE, Limits to ductility set by plastic flow localization, in "Mechanics of Sheet Metal Forming, eds. D.P. Koistinen and N.-M. Wang, Plenum Publishing Co., 237-265, 1978.

30. A. NEEDLEMAN and J.R. RICE, Plastic creep flow effects in the diffusive cavitation of grain boundaries, Acta Metall., 28, 1315-1332, 1980.

31. D. PEIRCE, R.J. ASARO and A. NEEDLEMAN, An analysis of nonuniform and localized deformation in ductile single crystals, Acta Metall., 30, 1087 - 1119, 1982.

32. P. PERZYNA, On material isomorphism in description of dynamic plasticity, Arch. Mechanics, 27, 473-484, 1975.

33. P. PERZYNA, Coupling of dissipative mechanisms of viscoplastic flow, Arch. Mechanics, 29, 607-624, 1977.

34. P. PERZYNA, Modified theory of viscoplasticity. Application to advanced flow and instability phenomena, Arch. Mechanics, 32, 403-420, 1980.

35. P. PERZYNA, Stability phenomena of dissipative solids with internal defects and imperfections, XVth IUTAM Congress, Toronto, August 1980 ; in "Theoretical and Applied Mechanics", Proc. eds. F.P.J. RIMROTT and B. TABARROK, North-Holland, Amsterdam, 1980, 369-374.

36. P. PERZYNA, Application of dynamical system methods to flow processes, Arch. Mechanics, 34, 1982 /in print/.

37. P. PERZYNA, Stability problems for inelastic solids with defects and imperfections, Arch. Mechanics, 33, 587-602, 1981.

38. P. PERZYNA, On constitutive modelling of dissipative solids for plastic flow, instability and fracture, International Conference on Constitutive Laws for Engineering Materials: Theory and Application, January 1983, TUCSON, Arizona.

39. P. PERZYNA and R.B. PĘCHERSKI, Modified theory of viscoplasticity. Physical foundations and identification of material functions for advanced strains, Arch. Meohanics, 35, 1983 in print.

40. R.B. PĘCHERSKI, Relation of microscopic observations to constitutive modelling for advanced deformations and fracture initiation of viscoplastic materials, Arch. Mechanics, 35, 1983 in print.

41. R.B. PĘCHERSKI, A note on contribution of dislocation generation and mobility to inelastic strain, Scripta Metall. submitted for publication.

42. M.R.D. RANDALL and J.D. CAMPBELL, Dynamic plasticity under combined stress. The development and use of medium-rate tension-torsion machine. University of Oxfort, Report No.1047, 1972.

43. J.R. RICE, The localization of plastic deformation, IUTAM Congress, Delft, August 1976; in "Theoretical and Applicol Mechanics, ed. W.T. Koiter, North-Holland, 207-220, 1976.

44. J.R. RICE, Time dependent fracture of materials at elevated temperature, ed. S. Wolf. p.130, U.S. Department of Energy Report CONF 790236 UC-25, Germantown, Md., June 1979.

45. M. SAJE, J. PAN and A. NEEDLEMAN, Void nucleation effects on shear localization in porous plastic solids, Int. Journ. of Fracture, 19, 163-182, 1982.

46. T. -L. SHAM and A. NEEDLEMAN, Effects of triaxial stressing on creep caviation of grain boundaries, Brown University Report, September 1982.

47. M.V. SPEIGHT and J.E. HARRIS, The kinetics of stress-induced growth of grain-boundary voids, Metal.Sci. J., 1, 83-85,1967.

48. V. TVERGAARD, On localization in ductile materials containing spherical voids, The Technical University of Denmark, Lyngby, Report 181, 1980.

49. J. WEERTMAN, Hull-Rimmer boundary voids growth theory - a correction, Scripta Metall., 7, 1129-1130, 1973.

50. J. WEERTMAN, Theory of high temperature intercrystalline fracture under static or fatigue loads, with or without irradiation damage, Metall. Trans., 5, 1743-1751, 1974.

51. P.J. WRAY, Strain-rate dependence of the tensile failure of polycrystalline material at elevated temperatures, J. Appl. Phys., 40, 4018-4029, 1969.